PNAS
www.pnas.org

Supplementary Information for

Cascade Degradation and Upcycling of Polystyrene Waste to High-Value Chemicals

Zhen Xu,[1] Fuping Pan,[1] Mengqi Sun,[1] Jianjun Xu,[2] Nuwayo Eric Munyaneza,[1] Zacary L. Croft,[1] Gangshu (George) Cai,[3] and Guoliang Liu*

Guoliang Liu

Email: *gliu1@vt.edu*

This PDF file includes:

Supplementary Information Text

I. Process Design for Techno-economic analysis (TEA) at an industrial scale

The TEA of PS waste was conducted at a scale of 100 tons/year and 1 ton/batch capacity.

1. Process design

A Sankey diagram demonstrates the major process streams and products (**Figure 4c**). A simple process flow diagram (PFD) is given in **SI Appendix, Figure S16.** The process is based on the following design:

(1) Production capacity, 100-ton PS per annum; batch reaction scale, 1 metric ton PS waste; operation time for each batch, 60 h.
(2) Degradation reaction conditions: UV light, ~37 ºC working temperature, 1 atm pressure, inert gas, and a reaction time of 24 h.
(3) Mass feed ratio: waste PS/benzene/$AlCl_3$ = 2/6/1.
(4) Benzene yield of PS degradation: 70 wt.% of the PS waste total mass (**SI Appendix, Table S1**).
(5) Mass of DCM used to upcycle 1 ton of PS waste: 1.0 t.
(6) Upcycling reaction condition: room temperature (~ 25 ℃), 1 atm, and 4 h.
(7) Upcycling conversion of DCM to DPM: 40 % (**SI Appendix, Figure S15b**)
(8) $H_2O/AlCl_3$ mass ratio for quenching: 1.4/1
(9) DPM mass fraction after removing the volatiles: 75 %
(10) Solvent loss, 2 wt.% (**SI Appendix, Figure S8**).

Note: The current process design can be further optimized. For example, adding a heat exchanger for fractional distillation can save energy and reduce production costs. However, it is omitted here, thus giving a relatively large utility cost (10% of the total production cost).

The process is separated into five steps: 1) degradation, 2) upcycling, 3) quenching, 4) chemical recovery, and 5) product separation. In the degradation step, PS waste is dissolved and degraded into benzene over $AlCl_3$ under UV. In the upcycling step, DCM is added to upcycle the primary degradation product benzene into DPM. By-product HCl is dissolved in refrigerated water, which is used as a quenching agent. After upcycling, the residual $AlCl_3$ can be reused to reduce $AlCl_3$ consumption in the next batch (**SI Appendix, Figure S3c**). Because $AlCl_3$ is hygroscopic, the amount of $AlCl_3$ residue depends on complex factors such as operation techniques and local climates. To simplify the TEA, residual $AlCl_3$ is quenched after Deg-Up and not reused in this workflow, resulting in a slight overestimation of the production cost. Prior to quenching, the light phase is removed. Then, the heavy phase is quenched by ice water (which may contain by-product HCl). In the chemical recovery step, the remaining DCM and benzene in the light phase are recovered by fractional distillation at atmospheric pressure. Finally, all products are separated via fractional distillation under reduced pressure. Among the products, light aromatics are distilled first and DPM is then collected, leaving heavy aromatics at the bottom of the distillation tower.

Degradation step. The designed PS degradation process is resilient to minor impurities like pigments, dirt, adhesives, and other plastics such as polyethylene, polypropylene, and polyvinyl chloride (see 10-g and 1-kg reactions), but $AlCl_3$ is sensitive to water and alcohols. Therefore, PS waste collected from municipal, packaging, or other sources should be pre-dried before dissolution in benzene and then degassed by a suitable method (*e.g.*, purging with N_2, ultrasonication, distillation, and freeze-pump-thaw). The PS solution and $AlCl_3$ fine powders are fed into an N_2-filled reactor through hoppers, followed by an N_2 flush to remove air and moisture that could be introduced during feeding. A UV lamp is then illuminated to initiate the degradation. The solution is agitated intensely to facilitate the reaction.

Upcycling step. N_2 gas flow and UV lamps are switched off in the upcycling reaction. Following the design, DCM is added to the reactor and stirred at room temperature for 4 h to obtain DPM. If it is necessary to accelerate the reaction and increase the conversion, the upcycling step can be conducted at higher temperatures.(1) The upcycling step is monitored by GC or other methods to ensure an equilibrium between the upcycled benzene and benzene extracted from PS waste. HCl is a gaseous by-product of upcycling, which is dissolved in chilled water for the quenching step.

Quenching step. The quenching is an exothermic reaction. Caution must be taken in a large-scale industrial reaction to prevent spilling and overheating. The light phase is removed prior to quenching. Acidic ice water is then added to the reactor to quench $AlCl_3$ and reactive species in the heavy phase. To ensure complete quenching, the molar ratio of water/$AlCl_3$ is at least 9 to 1. Acidic water is preferred because it hinders the formation of $Al(OH)_3$, an absorber of organic compounds. Therefore, the HCl solution obtained in the upcycling step is used. Quenching separates the heavy phase into layers of precipitates, water, and liquid organics. The solid precipitates are collected and combined with distillation residues to form a by-product of asphalt. The organic liquid is combined with the light phase for solvent recovery and product separation.

Chemical recovery step. The combined mixture is fractional-distilled to recover DCM and benzene. Due to the high volatilities of DCM and benzene (**SI Appendix, Table S4** and **Figure S17**), fractional distillation at room pressure is designed. The effect of light aromatics on the DCM-benzene distillation is ignored because of the huge volatility difference between the light aromatics and volatiles (20~50 times lower vapor pressure than volatiles, **SI Appendix, Table S4**). The designed purities for DCM and benzene are 93 wt. % and 99 wt. %, respectively.

Product separation step. After the recovery of DCM and benzene, the exhaust heat in the column is used for product separation. By fractional distillation at 10 mmHg, three products are separated: DPM, light aromatics, and heavy aromatics. DPM is the major product. Light aromatics (**SI Appendix, Table S4**) of C8~C10 hydrocarbons are separated first. As a naphtha oil, light aromatics have applications such as degreasing and plasticization. The remaining components in the column are DPM and heavy aromatics (**SI Appendix, Table S4**), which can be separated by fractional distillation again. The residual heavy aromatics have high boiling points and are combined with the precipitates from the quenching step to form asphalt.

2. Key equipment design

Based on the PFD (**SI Appendix, Figure S16**), the primary equipment and accessories, including reactor, UV light source, distillation column, and vacuum pump, are designed at a 1-ton scale. The equipment and accessories are utilized for equipment cost evaluation and TEA.

UV light power and reactor design.

The power of UV light and the number of light bulbs needed for the 1-ton PS degradation is estimated based on the 1-g and 1-kg PS reactions. Generally, the number of photons ($n_{/s}$) generated by one UV lamp within a unit of time is defined by **SI Appendix, Equation S1**,

$$n_{/s} = \frac{p_{ex} \times A \times \lambda_{ex}}{hc} \quad \text{(S1)}$$

where p_{ex} is the illumination power density (0.0125 W cm^{-2}), A is the illumination area (120 cm^2), λ_{ex} is the illumination wavelength (253.7 nm), h is Planck's constant, and c is the speed of light. Considering the illumination time (t) and the number of UV light bulbs used ($N = 12$), the numbers of photons needed (n) for degrading 1-g ($n_{1\,g}$) or 1-kg ($n_{1\,kg}$) of PS can be calculated (**SI Appendix, Table S5**) as follows.

$$n = n_{/s} \times N \times t \quad \text{(S2)}$$

To relate the total number of photons generated to the mass of PS (m_{PS}), two parameters apparent quantum efficiency (φ) and PS degradation pre-factor ($\boldsymbol{\varepsilon}$) are introduced:

$$n \times \varphi = n_{eff} = m_{PS} \times \varepsilon \quad \text{(S3)}$$

where n_{eff} is the number of photons effectively used in the reaction, φ is the apparent quantum efficiency that describes the ratio of the effective photons in the reaction to the total number of photons generated by the lamp and it can vary depending on the experimental conditions. ε is the PS degradation pre-factor; it represents the number of photons needed for degrading PS and is intrinsic to the reaction mechanism.

The apparent quantum efficiency φ is difficult to quantify but can be approximated to be dependent on the mass of the PS, because of an increasing mass of PS benefits photons usage. Apparent quantum efficiency for 1000 times mass increment ($\varphi_{1000/1}$) can be calculated based on

the up-scaling from 1 g to 1 kg. Thus, the apparent quantum efficiency for 1000 times scale-up can be expressed as,

$$\boldsymbol{\varphi_{1000/1}} = \frac{\boldsymbol{\varphi_{1000g}}}{\boldsymbol{\varphi_{1g}}} = \frac{\boldsymbol{\varepsilon \times (1\ kg)/n_{1\ kg}}}{\boldsymbol{\varepsilon \times (1\ g)/n_{1\ g}}} \quad \text{(S4)}$$

$\varphi_{1000/1}$ is estimated to be similar to that between 1-ton and 1-kg reaction. Thus, the total photon number needed for 1-ton PS degradation can be estimated (**SI Appendix, Equation S5**),

$$\boldsymbol{\varphi_{1000/1}} = \frac{\boldsymbol{\varphi_{1\ ton}}}{\boldsymbol{\varphi_{1\ kg}}} = \frac{\boldsymbol{\varepsilon \times (1\ ton)/n_{1\ ton}}}{\boldsymbol{\varepsilon \times (1\ kg)/\ n_{1\ kg}}} \quad \text{(S5)}$$

Finally, the number of required photons generated is used to find the number of UV-C light bulbs ($90\ \mu W/cm^2\ at\ 1\ m\ distance$) needed for 1-ton PS degradation ($N_{1\ ton}$), assuming the reaction time is 24 h (**SI Appendix, Equation S6** and **Table S5**).

$$\boldsymbol{N_{1\ ton}} = \frac{\boldsymbol{n_{1\ ton}/t_{1\ ton}}}{\boldsymbol{n_{/s}}} \quad \text{(S6)}$$

The volume of the reactor is evaluated based our optimized process for larger-scale reactions. An extra 20% space is given for safety concerns. The evaluation result is tabulated in **SI Appendix, Table S6**.

Distillation column design.

The distillation column is used to perform two separation processes: (A) chemical recovery and (B) product separation. The column dimension is determined by the more-demanding process that requires more plate number, tower height, tower width, and wall thickness. The design of the distillation column follows a recommended procedure in an international standard (ASME BPV Sec. VIII D.1 Part UG-28) and literature.(2, 3) Details of the design are exhibited as follows.

A. Chemical recovery process. The fractional distillation column is first used to recover DCM and benzene from the reaction mixture.

Flow rates. DCM and benzene are much more volatile than the rest chemicals in the product mixture containing light aromatics, DPM, and heavy aromatics (**SI Appendix, Table S4**). Therefore, to simplify the design of plate number and size, the feed is regarded as a binary mixture of DCM (light component) and benzene (heavy component). Based on the Deg-up reaction at the 1-kg scale, the fractions of DCM and benzene in a 1-ton reaction are assumed to be ~ 17 wt.% and 83 wt.% (**SI Appendix, Figure 4c**), respectively. The purities of DCM and benzene are designed to be 93 wt.% and 99 wt.%, respectively. Total distillate flow rate (D) and bottom flow rate (B) are calculated based on the following equations and the results are tabulated in **SI Appendix, Table S6**

$$\begin{gathered}\boldsymbol{F \times Z_F = x_D \times D + x_B \times B} \\ \boldsymbol{F = D + B}\end{gathered} \quad \text{(S7)}$$

where *F* is the feed flow rate, Z_F is the fraction of light components in the feed, x_D is the fraction of light components in the distillate, and x_B is the fraction of light components in the bottom.

Minimal plate number. The vapor pressures of DCM and benzene at various temperatures are calculated according to the NIST database (**SI Appendix, Figure S17a)**. The dew point of the distillate, as well as the bubble point of the bottom, is determined using an iterative method based on vapor pressure at varying temperatures.(2, 4) At 760 mmHg, the Dew point temperature is ~41 ºC (column top), the bubble point temperature is ~79 ºC (column bottom), and the feed boiling point is 69 ℃. The relative volatilities (α) are determined based on the vapor pressures at the Dew and bubble point temperatures under 760 mmHg (**SI Appendix, Equation S8** and **Figure S17a**). (1-7)

$$\boldsymbol{\alpha = P_L^*/P_H^*} \quad \text{(S8)}$$

where P_L^* is the vapor pressure of the light component; P_H^* is the vapor pressure of the heavy component; α is the relative volatility. The overall relative volatility of the entire process is assumed to be the geometric average of the relative volatilities at the column top and bottom (**SI Appendix, Table S6**).

The minimal plate number is evaluated using Fenske equation (**SI Appendix, Equation S9**)(2)

$$\boldsymbol{N_{min} = \frac{\log\left[\frac{x_L}{x_H}\right]_d\left[\frac{x_H}{x_L}\right]_b}{log\alpha_{AD}}} \quad \text{(S9)}$$

where N_{min} is the minimal plate number, $[\frac{x_L}{x_H}]_i$ is the fraction ratio of the light and heavy components in distillate (d) or bottom (b). The result was tabulated in **SI Appendix, Table S6**.

The actual plate number is evaluated based on the column efficiency using O'Connell's correlation (**SI Appendix, Equation S10**).(2)

$$\boldsymbol{E = 51 - 32.5log(\mu \times \alpha)} \quad \text{(S10)}$$

where *E* is column efficiency and μ is liquid molar average viscosity (mN s/m^2),(8)

The minimal reflux ratio is evaluated using the Underwood equation (**SI Appendix, Equations S11 and S12**).(2) As the feed is at its boiling point (69 ℃, 760 mmHg), the Underwood equation can be rewritten as follows to find out the factor θ,

$$\boldsymbol{\sum \frac{\alpha_i x_{i,f}}{\alpha_i - \theta} = 0} \quad \text{(S11)}$$

where α_i is the average relative volatility; $x_{i,f}$ is the component concentration in the feed, θ is a constant and equals 2.57 for the DCM-benzene recovery.

The minimal reflux ratio is then calculated using θ and **Equation S12** in **SI Appendix**,

$$\boldsymbol{\sum \frac{\alpha_i x_{i,d}}{\alpha_i - \theta} = R_{min} + 1} \quad \textbf{(S12)}$$

where $x_{i,d}$ is the component concentration in distillate; $\theta = 2.57$; R_{min} is the minimum reflux ratio. The results are tabulated in **SI Appendix, Table S6**. The actual reflux ratio (R) is evaluated by multiplying a factor of 1.5.

Minimal plate diameter evaluation. The diameter of the plate depends on the upper limit of vapor velocity (u_v) and vapor flow rate (V). The vapor velocity must be adequately low to prevent excessive liquid entrainment or high pressure drop.(3) In this work, u_v is estimated using the long-established empirical Fair Equation(2) (**SI Appendix, Equation S13)** and the results are tabulated in **SI Appendix, Table S6**.

$$\boldsymbol{u_v = K_v \sqrt{\frac{\rho_L - \rho_V}{\rho_V}} (\frac{\sigma}{20})^{0.2}} \quad \textbf{(S13)}$$

where K_v is an empirical coefficient determined by a diagram method;(3) assuming a plate distance of 0.2 m, K_v is ~ 0.17 for the DCM-benzene recovery system; ρ_L and ρ_V are densities of the liquid and vapor, respectively; σ is the surface tension and a value of σ = 20 dyn/cm is selected, which is typical for organic liquids.(3)

To evaluate the vapor densities (**SI Appendix, Table S6**), the average molecular weight of vapor is calculated using the ideal gas equation, based on the ratio of vapor pressure between DCM and benzene at 69 ºC (**SI Appendix, Equation S14**). The liquid phase is evaluated using the data of benzene (**SI Appendix, Table S4**), due to the dominance of benzene in the liquid.

$$\boldsymbol{\rho_v = \frac{PM_v}{RT} = \frac{x_H v_H M_H + x_L v_L M_L}{RT}} \quad \textbf{(S14)}$$

where v is the vapor pressure of the light (DCM) and heavy components (benzene) at the boiling point of the mixture; x_i is the molar ratio of the heavy (x_H; $x_{Ben} = 0.83$) and light components (x_L; $x_{DCM} = 0.17$), respectively; P is the pressure; R is the ideal gas constant; *T* is the boiling point of the mixture; M_i is the molar mass of the light (DCM) and heavy components (benzene).

Vapor flow rate (*V*, m^3/s) is calculated based on mass balance (**SI Appendix, Equation S15**).

$$\boldsymbol{V = (R_{actual} + 1)D/3600 \times \rho_v)} \quad \textbf{(S15)}$$

Minimal column area, or bubbling area is calculated using **SI Appendix, Equation S16**.

$$\boldsymbol{A_{min} = V/u_v} \quad \textbf{(S16)}$$

where A_{min} is the minimal column area. The actual area is calculated based on a factor of 2 than the minimal area (**SI Appendix, Table S6**).

B. DPM separation process.

Flow rates. Based on the 1-kg scale experiment (**Figure 4**), the fractions of light aromatics, DPM, and heavy aromatics for a 1-ton scale reaction are evaluated to be ~ 11 wt.%, ~ 75 wt.%, and ~ 14 wt.%, respectively (**Figure S12**). Heavy aromatics are difficult to be distilled due to the low volatility and high boiling point (**SI Appendix, Table S4** and **Figure S18**). Therefore, the feed is regarded as a pseudo-binary mixture of DPM (heavy component) and light aromatics (light component) with

a mass ratio of 75:11. The feed is approximated to be 1 ton. The separation is designed to yield light aromatics and DPM with purities of 97 wt.% and 99 wt.%, respectively. Similar to the chemical recovery process, the total distillate amount (D) and bottom amount (B) are calculated based on **Equation S7** in **SI Appendix**.

Minimal plate number evaluations. Because the actual composition of the light aromatics is too complicated to be determined, 1-methyl indene is selected to represent the light aromatics because 1) physiochemical properties of 1-methyl indene can be easily predicted by the Antoine equation or found from physiochemical handbooks; 2) 1-methyl indene is the least volatile compound among the light aromatics produced in our reactions. Therefore, the removal of 1-methyl indene ensures the removal of other light aromatics.
Vapor pressure of 1-methyl indene is calculated using the Antoine equation (**SI Appendix, Equation S17**).

$$logP = A - \frac{B}{T + C} \quad \textbf{(S17)}$$

where the Antoine constants A=7.10152, B=1711.34, and C=206.962 for 1-methyl indene; T is the temperature (℃); *P* is vapor pressure (mmHg).

To reduce the temperature requirement and prevent coking, the distillation is operated at a reduced pressure of 10 mmHg. Under this condition, the Dew point of the distillate and the bubble point of the bottom are determined using an iterative method based on vapor pressure data at different temperatures (**SI Appendix, Figure S17b**).(2, 4) At 10 mmHg, the Dew point temperature is 74 ºC (column overhead); the bubble point temperature is 124 ºC (column bottom); the feed boiling point is 108 ℃.

The relative volatilities (α) at dew and bubble point temperatures are determined based on the vapor pressures under 10 mmHg (**SI Appendix, Equation S8**).

The minimal plate number is evaluated using the Fenske equation (**SI Appendix, Equation S9**). The actual plate number is evaluated based on the column efficiency using O'Connell's correlation (**SI Appendix, Equation S10**). Because of the dominance of DPM, the molar average liquid viscosity (mN s/m^2) is approximated to the viscosity of DPM at 108 ℃.(8)

The minimal reflux ratio is evaluated using the Underwood equation (**SI Appendix, Equations S11 and S12**). As the feed is at its boiling point (108 ℃, 10 mmHg), the constant θ for DPM separation is calculated to be 4.6. The minimal reflux ratio is calculated using $\theta = 4.6$ and **Equation S12** in **SI Appendix**. The actual reflux ratio is evaluated by multiplying a factor of 1.5.

Minimal tray diameter. The u_v for DPM separation is estimated using **Equation S13** in **SI Appendix.** The vapor density is calculated using the ideal gas equation and average molecular weight (**SI Appendix, Equation S14**). Assuming a plate distance of 0.2 m, the constant K_v for DPM separation is ~ 0.18.(2, 3) the density of the liquid at the column top and bottom is approximate to that of DPM (**SI Appendix, Table S4**), due to the similar densities of 1-methyl indene and DPM. The results are tabulated in **SI Appendix, Table S6**.

Vapor flow rate (m^3/s) is calculated based on mass balance (**SI Appendix, Equation S15**). The minimal bubbling area is calculated using **Equation S16** in **SI Appendix**. The actual area is calculated based on a factor of 2 than the minimal area (**SI Appendix, Table S6**).

Distillation column dimension.
Tower height. Assuming a plate distance of 0.2 m, the height of the column is calculated using the process requiring the most plates, *i.e.*, DPM separation.
Tower diameter. The tower diameter is calculated using the process requiring the largest plate diameter, *i.e.*, DPM separation.
Column wall thickness. The column wall thickness is evaluated using Figure G and Figure CS-2 in ASME BPV Sec. VIII D.1 Part UG-28 standard. The external pressure applied for thickness evaluation is 15 psi (absolute vacuum) instead of the designed 10 mmHg to ensure safety. An extra 2 mm is designed for weathering. All tower dimension results are tabulated in **SI Appendix, Table S6**.

Vacuum pump design
The vacuum pump is selected based on its vacuum capacity and maximum vacuum. The vacuum capacity is expected to be > 2.52 m^3/h to ensure the design vacuum is reached within an hour. The vacuum should be better than 29.5 inHgV (10 mmHg).

II. Techno-economic analysis of PS Deg-Up to DPM

1. Assumptions for TEA at an industrial scale

Key capital investment assumptions (**SI Appendix, Table S7)** are adapted from Peters *et al.* (2003) and Towler and Sinnott (2007).(2, 9) Other critical assumptions used in the basic scenario are tabulated in **SI Appendix, Tables S7 and S8,** including project length salvage value, depreciation method and period, annual interest rate, fixed costs (raw materials and product prices), operating labor, operating supervision, utilities, maintenance and repairs, operating supplies, laboratory charges, royalties, plant overhead costs, and general expenses. In our TEA the scale is assumed to be 100 t/y, which is 10% of the current global demand for DPM in the fragrance, pigment, and pharmaceutical industries.(10) However, a larger annual scale, such as 10,000 t/y, can be designed because DPM has a large downstream market of benzophenone, a potential PS Deg-Up product (**Figure 4e**) that has a demand of 61,760 t/y in 2021.(11) The market size of benzophenone is projected to be doubled by 2027.(12)

2. Chemical price analysis.

The cost of crude oil was based on the West Texas Intermediate (WTI) petroleum price in 2021 ($83.57/bbl, Nov. 1st). The styrene and PS prices were from Statista®. The PS waste price was based on the highest price (LA1300970, $0.8/lbs, March 15th, 2021) reported on the global recycling network (GRN) for condensed EPS blocks. The benzene price was from Platts Global Benzene Price Index (March 18th, 2021), and the cumene, toluene, and dichloromethane prices were from Echemi market price & insight (May 10th, 2021). Diphenylmethane and benzophenone prices were based on the average prices in the market investigations.(10, 13)

The PS waste price depends on many factors, including collection, transportation, and storage because PS is sometimes used as expanded foams and has a high volume/mass ratio. In addition, due to regional disparities in labor, infrastructures, and facilities, these costs cannot be precisely evaluated like petroleum and other bulk chemicals. Thus, we have used prices of regenerated PS powders, granulates, and beads in the TEA, which in principle includes all the costs to collect and process PS wastes.

The regenerated PS prices are collected from online wholesale markets, including 87 data points from 15 countries. The price distribution is summarized in **SI Appendix, Figure S25**. We have selected the price of ~ $800/t for the following TEA analysis. The actual cost of our feedstock PS waste should be lower than the regenerated PS powders, granulates, and beads. The regenerated PS powders, granulates, and beads can be easily traded and transported to our upcycling sites.

3. Capital investment

Based on the process design and PFD (**SI Appendix, Figure S16**), we estimate the fixed-capital and total capital investment using the method of Percentage of Delivered-Equipment Cost. The size of the photoreactor, number of UV light bulbs, distillation tower dimensions, plate dimensions, and vacuum pump performance are designed to establish a preliminary industrial process. The equipment cost is evaluated using the cost curve method based on the factors in key equipment design (**SI Appendix, Tables S5** and **S6**).(2) The evaluation results are summarized in **SI Appendix, Table S9**. Other items including the total direct plant cost are estimated as percentages of the delivered-equipment cost. The additional components of the capital investment are based on average percentages of the total direct plant cost, total direct and indirect plant costs, or total capital investment.(9)

4. Product cost and revenue

Total product costs include manufacturing costs and general expenses. Manufacturing costs include all expenses directly connected with the manufacturing operation or the physical equipment of a process plant itself, including variable production costs, fixed charges, and plant overhead

costs. We first estimate the raw material cost and then other direct production costs as a percentage of the total product cost or of the labor cost.(9) The raw material cost was evaluated based on the chemical inputs and chemical prices in 2021 (**SI Appendix, Table S8**). For 1 ton of PS waste, the degradation-upcycling process requires 3 tons of benzene, 0.5 tons of $AlCl_3$, and 1 ton of DCM. The theoretical DPM output of recycling 1-ton PS waste is 0.75 tons.

Fixed charges include depreciation, local taxes, insurance, rent, and financing interest.(9) Normally they are affected by fixed capital investment and are estimated to be 10%—20% of the total product cost.(9) Plant overhead costs may include general plant upkeep and overhead, payroll overhead, packaging, medical services, safety and protection, restaurants, recreation, salvage, laboratories, and storage facilities. Normally they take 5%—15% of the total product cost. General expenses refer to administrative costs, distribution and selling costs, and research and development costs. Normally they are about 15%—25% of the total product cost.

Gross earnings are calculated by total revenue minus total product cost. Revenue comes from sales of products produced by the plant. The total annual revenue from product sales is the sum of the unit price of each product multiplied by its rate of sales ($/yr = $\sum(\text{sales of product, ton/yr})$(product sales price, $/ton)).

5. Profitability

The calculation of profitability is performed with four measures that can be classified into two groups, depending on whether the time value of money is considered. The methods that do not consider the time value of money include return on investment (ROI) and payback period (PBP). The methods that consider the time value of money include net present value (NPV) and internal rate of return (IRR). The NPV combined with IRR, is strongly recommended for making economic decisions.(9)

ROI is defined as the ratio of profit to investment (**SI Appendix, Equation S18**).

$$\mathrm{ROI} = \frac{\text{annual net profit}}{\text{total capital investment}} \tag{S18}$$

Net profit usually is not constant from year to year; the recommended approximation is to take the average ROI over the entire project life.

PBP is the length of time needed for the total return to equal the capital investment (**SI Appendix, Equation S19**).

$$\mathrm{PBP} = \frac{\text{fixed capital investment}}{\text{average annual cash flow}} \tag{S19}$$

where the total project generated cash flow (**SI Appendix, Equation S20**) returned to the capital reservoir on an annual basis is as follows.

$$\mathrm{A_j} = (\mathrm{s_j} - \mathrm{c_{oj}})(1 - \Phi) + \mathrm{d_j}\Phi \tag{S20}$$

where A_j is the cash flow from the project to the corporate capital reservoir resulting from the operation in year j, s_j the sales rate in year j, c_{oj} the cost of operation (depreciation not included) in year j, d_j is the depreciation charge in year j, and Φ the fractional income tax rate.

Here, we use the straight-line method to calculate depreciation (**SI Appendix, Equation S21**). In this method, the property value is assumed to decrease linearly with time over the recovery period. No salvage may be taken.

$$\text{Annual depreciation} = \frac{\mathrm{OPI}}{\mathrm{LRP}} \tag{S21}$$

where OPI is the original property investment at the start of the recovery period, LRP is the length of the straight-line recovery period.

NPV is the total of the present value of all cash flows minus the present value of all capital investments (**SI Appendix, Equation S22**). NPV is calculated based on nominal net cash flow A_j at year *j*; *r* is the discount rate; *n* is the lifetime; and TCI refers to total capital investment, defined as follows.

$$\mathrm{NPV} = \sum_{\mathrm{j}=1}^{\mathrm{n}} \frac{\mathrm{A_j}}{(1+\mathrm{r})^{\mathrm{j}}} - \mathrm{TCI} \tag{S22}$$

IRR is defined as any discount rate that results in an NPV of zero. Thus, it is determined by setting the NPV given by **SI Appendix, Equation S22** equal to zero and solving for the discount rate that satisfies the resulting relation.

6. Results of TEA at an industrial scale for PS Deg-Up

The TEA is conducted based on a 100-ton/year waste PS capacity. For the base scenario, the fixed capital expense is calculated at $1.11M. Among them, 27% are contributed from purchased equipment, 42% from other direct costs, and 31% from indirect costs. The total capital investment is thus about $1.28M, including $0.17M working capital.

Assuming 100% capacity, annual sales are $0.765M. The annual product cost without depreciation is $0.414M. This leads to an annual gross profit of $0.35M, and an annual net profit of $0.221M. This results in an IRR of 22.75%, a payback time of 4.49 years, and an average return of investment of 17.25%. This outcome is significantly better than the extant approaches that are generally unprofitable.

Sensitivity analysis. We conduct sensitivity analyses to evaluate how changes in several design and cost assumptions affect the overall profitability. **SI Appendix, Figure S19** shows the tornado diagram in which the deviation in the IRR is plotted when varying a single parameter, compared to the basic scenario defined above.

The IRR for the basic case is 22.75%, resulting in a payback time of 4.49 years and an ROI of 17.25%. The biggest impact on the IRR and PBP results from the variation of the DPM output, DPM price, and equipment cost. If the DPM output or the DPM price decreases by 30%, the IRR will decrease to 6.48%. If the equipment cost increases by 30%, the IRR will decrease to 13.27%. On the other hand, if the DPM price or DPM output increases by 30%, the IRR increases to 36.77%. If the equipment cost drops by 30%, the IRR increases to 35.05%. Note that changing DPM price and output has the same impact on profitability. This is not surprising, because they have the same directional effect on revenue.

The overall profitability shows less sensitivity to other inputs. For example, when increasing or decreasing the waste PS price by 30%, the IRR decreases to 19.83% or increases to 25.61%, respectively; when increasing or decreasing the aromatics price by 30%, the IRR only increases to 22.94% or decreases to 22.46%. This insensitivity is due to the fact that aromatics only contributes a small percentage of the revenue compared to DPM. The changes in IRR compared with that in DPM are illustrated in **SI Appendix, Figure S20**.

We change the percentage of operating labor and utility in the total product cost from 10% to 20% (**SI Appendix, Figure S21**). Labor cost and utility show similar patterns of little sensitivity, with IRR decreasing slightly from 25% to around 20%.

Theoretical atom efficiency and process modification. Theoretical atom efficiencies of the presented process (**Figure 4**) are estimated by molar and weight. The organics consumption and yield during the degradation and upcycling are considered in the estimation, including PS (1.0 ton, 158,415 mol atoms), DCM (0.42 ton, 24705 mol atoms), benzene (0.06 ton, 9928 mol atoms), DPM (0.75 ton, 110946 mol atoms), naphtha oil (0.11 ton), and asphalt (0.14 ton). Along with the upcycling to DPM, by-product HCl (19764 mol atoms) is generated from DCM. If the process is well-controlled with no leaking, the atom efficiency by molar is 90%. The 10 mol% loss is attributed to the chlorine atoms in DCM.

Atom efficiency can also be calculated by weight. Based on the input and output, the atom efficiency of the process is 67 wt. %. Again, the lost efficiency is attributed to DCM composed primarily of chlorine (Cl wt.% = 84 %).

Two methods can be implemented industrially to obtain a better atom economy. First, if the investor wants to use DCM for PS Deg-Up, the released HCl can be absorbed by water to generate diluted HCl solutions for use as a household cleaning product. Second, DCM can be replaced by benzyl chloride (Cl wt. % = 28 %). DPM is industrially prepared by the Friedel–Crafts alkylation of benzyl chloride with benzene in the presence of a Lewis acid such as aluminum chloride. The theoretical atom efficiency of the industrial method is 83% by mass.

III. Techno-economic analysis of PS decomposition to styrene (PDS)

Decomposition of PS into styrene can give monomers for synthesizing regenerated PS and has attracted interest in the industry. To compare it with our Deg-Up method, we have conducted TEA for PDS.

1. Key process design and assumptions

To construct a PS decomposition process flow for TEA, we have referred to the Agilyx patent.(14) The PS decomposition process consists of two major sections: 1) PS waste degradation in a pyrolysis reactor; 2) styrene oil purification through a condensation system, including an immiscible liquid condenser and several water condensers. The styrene oil is then polymerized into PS through bulk polymerization. To give the most favorable consideration to the PDS process, we have used highly optimistic assumptions for the PS decomposition process:

1. The cost of catalyst is assumed to be zero;
2. The yield of styrene is assumed to be 99 %;
3. Bulk polymerization is assumed for the repolymerization process, which avoids the need for solvents;
4. The cost of the initiator is ignored due to the small usage in a typical polymerization process;
5. The conversion of styrene to PS is assumed to be 100 % (the best possible situation);
6. Processing cost (including the processing device, labor, and energy) on the PS is assumed to be zero;
7. No external subsidy or tax reduction is provided to the company to ensure full self-sustainability.

2. Key equipment design

Based on the above process flow and an annual capacity of 10000, 1000, and 100 tons, we have evaluated the cost of primary equipment, including a static mixer, pyrolysis reactor, and polymerization reactor. We have chosen a capacity of 10000 t/y because it is the typical capacity claimed by companies (*e.g.,* Ineos and Agilyx). Annual capacities of 1000 and 100 tons are also included to investigate the effect of production scale on the business model. Other equipment and accessory costs are assumed to be ~30% of the total equipment cost.

Static mixer. Following the process disclosed by available companies, we have used a continuous mode for PDS rather than the batch mode in our PS Deg-Up process. The reactor size depends on the feeding rate of the mixer. A capacity of 2.1 kg/s is required to complete the pyrolysis within 3.6 h and reach the daily capacity of 27 tons/day. The PS wastes go through thermal densification in the disclosed process,(14) and the resulting PS melt is injected into the pyrolysis reactor. Assuming a density of 1 kg/L for the PS melt, the volumetric capacity of the mixer should be > 2.1 L/s. Similarly, the mixer capacities of 1000 t/y and 100 t/y are determined to be 0.21 L/s and 0.021L/s, respectively.

Pyrolysis reactor. The disclosed process requires a pyrolysis temperature of near 550 ℃ (1000 ℉). According to a pilot experiment of a similar PS pyrolysis process,(15) a residence time of 0.7 h is needed under 550 ℃ and atmospheric pressure. Assuming the same residence time, PS in the reactor is approximately 5.1 m^3 under the designed feeding ratio (2.1 L/s). If we design an extra 20% space for safety, the pyrolysis reactor should be > 6.5 m^3. Similarly, the reactor volumes for the 1000 and 100 t /y processes are determined to be >1 m^3 and > 0.5 m^3, respectively.

Polymerization reactor. If the recycled styrene is repolymerized using free-radical bulk polymerization, one may follow Dow's patent on PS bulk polymerization and complete polymerizing 27-ton styrene in one pot (US35571694A, expired). With an extra 20% space for safety, the polymerization reactor should be > 34 m^3. Similarly, the reactor volumes for the 1000- and 100-t/y processes are determined to be > 3.3 m^3 and > 0.5 m^3, respectively.

3. Key TEA assumptions

The TEA of PS decomposition to styrene adapted the same key capital assumptions to the PS Deg-Up above (**SI Appendix, Tables S7 and S8)**. The main product in PDS is regenerated PS, and it is assumed to have a value of $1500/t in the basic scenario.

Capital investment: We estimate the fixed-capital and total capital investment using the method of Percentage of Delivered-Equipment Cost. The capacity of the static mixer, the volume of the pyrolysis reactor, and the size of the polymerization reactor are designed to estimate the equipment cost of the disclosed industrial process. The evaluation results are summarized in **SI Appendix Table S9**. Other items, including the total direct plant cost and additional components of the capital investment, are estimated similar to that in the PS Deg-Up process.

Product cost and revenue: The estimation methods for total product costs and gross earnings are similar to the PS Deg-Up process. Because the PDS process requires no extra additives, the output of the regenerated PS is optimistically assumed to be 1 ton if the input is 1 ton of PS waste, which is an ideal situation.

Profitability: The profitability (i.e., ROI, IRR, and PBP) of the PS decomposition to styrene process is investigated using **SI Appendix Equation S18-22**.

4. Key TEA Results for PDS

Our TEA suggests a fixed capital expense of $2.46M for a process with an annual capacity of 10000-ton PS waste. Without external subsidy or tax reduction, TEA shows that the process is not profitable if the prices of PS waste and regenerated PS are $800/t and $1500/t, respectively. Both profit and cash flow are negative, giving a deficit of $280k in the first year. The business must either reduce the PS waste cost or increase the regenerated PS sale price to be profitable.
In addition, the PDS process shows the following features:

1) PDS is strongly sensitive to the PS and PS waste prices.

Sensitivity analysis shows that profitability strongly depends on virgin PS and PS waste prices (**SI Appendix, Figures S19** and **S22**). On a scale of 10000 t/y, if the virgin PS price is at $1500/t, which is the highest price of PS in the recent five years, PDS must control the PS waste cost to be < $778/t to be profitable. If the PS is sold at $1200/t, the recent-5-year average price, the PS waste cost must be < $616/t (**SI Appendix, Figure S22b**). However, in our price investigation (**SI Appendix, Figure S25**), only 29% of the reported prices are < $616/t. The tornado diagram (**SI Appendix, Figure S19b**) also illustrates the strong sensitivity to the PS waste and regenerated PS prices. The prices of PS waste and regenerated PS in the tornado diagram are preset to $600/t and $1500/t, respectively, due to the negative profit and cash flow in the basic scenario. Upon increasing or decreasing the PS waste price by 30%, the IRR decreases 100% or increases 77%, respectively, suggesting a deficit of $93k or a net profit of $6 M, respectively. Similarly, upon increasing or decreasing the regenerated PS price by 30%, the IRR decreases 100% or increases 126%, respectively, indicating a deficit of $12k or a net profit of $8M.

2) The sensitivity and profitability depend on the production scale.

Reducing the annual capacity considerably reduces the sensitivity to the PS prices (**SI Appendix, Figure S23**), but it also sharply reduces profitability due to the small price difference between PS waste and the regenerated PS.

The TEA results partially explain the typical trial scale of 10 t/d by new recycling companies (*e.g.,* Agilyx Tigard, in Oregon and New Hampshire) because a production capacity in the range of 1000 – 10000 t/y has better resistance to market fluctuation and acceptable profitability. Large production scales are possible if the business has adequate control over the PS waste and product prices (e.g., Ineos Styrolution has invested in a facility in Channahon, Illinois, with a capacity of 100 t/d.)

IV. Advantages of Deg-Up compared with PDS

The Deg-Up process is complementary to the existing plastic recycling technologies. As a plastic upcycling strategy, it converts plastic wastes to high-value products and has the following advantages:

1) **Resistant to market fluctuation.** Compared with PDS, Deg-Up is much less sensitive to market fluctuation, especially the prices of PS and PS wastes and the costs of waste collection, transportation, and storage. This characteristic makes Deg-Up attractive to regions where infrastructures are underdeveloped, and costs of waste collection/transportation, labor, and energy are high. An increase in the PS waste cost by 50% from $800/t to $1200/t only slightly reduces the IRR in our PS Deg-Up process.
2) **Versatile and diverse upcycling products.** Unlike PDS which converts PS wastes to monomers and regenerated PS with comparable prices to the virgin PS, Deg-Up can produce a diverse series of high-value products. Switching the added chemicals in the upcycling step generates new products to satisfy the varying market needs. For example, adjusting the upcycling reactions can convert PS wastes to triphenylmethane, 1,2-diphenylethane, diphenylketone, 1,4-dibenzylbenzene, and 4-phenyl-4-oxo butyric acid (**Figure 4e** and **SI Appendix, Figure S24**).
3) **Compatible with existing industrial processes.** Deg-Up is compatible with existing industrial processes and can be easily adopted by the industry. For example, our designed PS Deg-Up to DPM is similar to the existing industry of DPM production, where benzyl halide reacts with benzene over $AlCl_3$. Our Deg-Up process simply replaces benzyl halide and benzene with PS waste and DCM, while all processes and even by-products are similar (**SI Appendix, Figure S26**).

Despite these advantages, Deg-Up is not intended to replace the existing recycling technologies. As an upcycling strategy, it does not circulate plastics in society as mechanical recycling does. It is most suitable for eliminating “end-of-life” plastics that can no longer be regenerated. Additionally, in consideration of market sizes, it is necessary to expand the use of Deg-Up for producing large-volume chemicals such as surfactants, food additives, disinfection products, and paint. In short, as a versatile strategy with good industrial compatibility, profitability, and resistance to market fluctuation, Deg-Up is attractive to new players in the plastic recycling industry. It has the potential to work together with other methods and address the plastic pollution crisis.

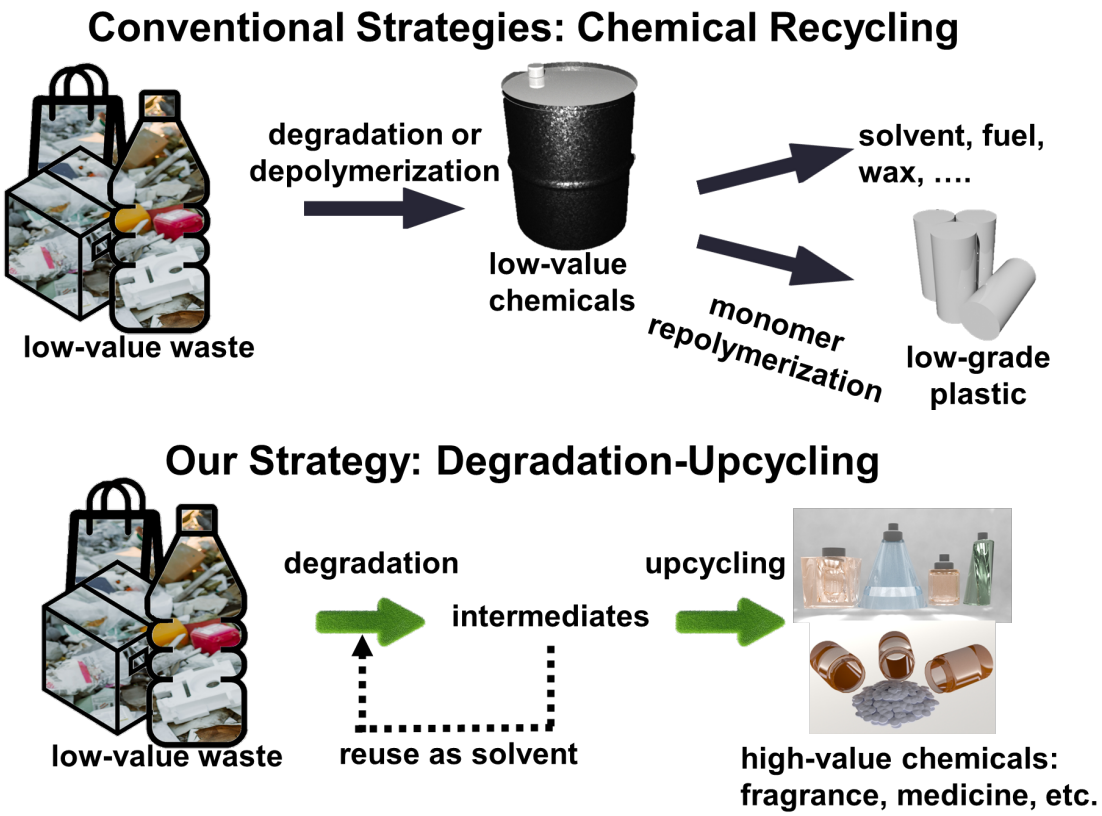

Figure S1. Comparison of plastic recycling and upcycling strategies. (top) Conventional recycling strategies: Plastic wastes are degraded or depolymerized into low-value chemicals such as solvents, fuels, waxes, or monomers. Monomers can be repolymerized to produce plastics but often of a lower grade and lower value. (**bottom**) **Our tandem Deg-Up strategy:** Plastic wastes are upcycled into a high-value product following two steps in one reactor vessel using the same catalysts. Plastic wastes are first degraded into intermediates using non-precious metal catalysts under mild reaction conditions. Subsequently, the intermediates are upcycled and valorized into high-value chemicals. In this work, PS waste was first degraded over $AlCl_3$ under UV exposure into aromatic intermediates (primarily benzene). The recovered benzene was upcycled to high-value diphenylmethane. The leftover benzene intermediate can be reused as a solvent for the next degradation cycle, forming a self-sustainable circuitry of plastic valorization.

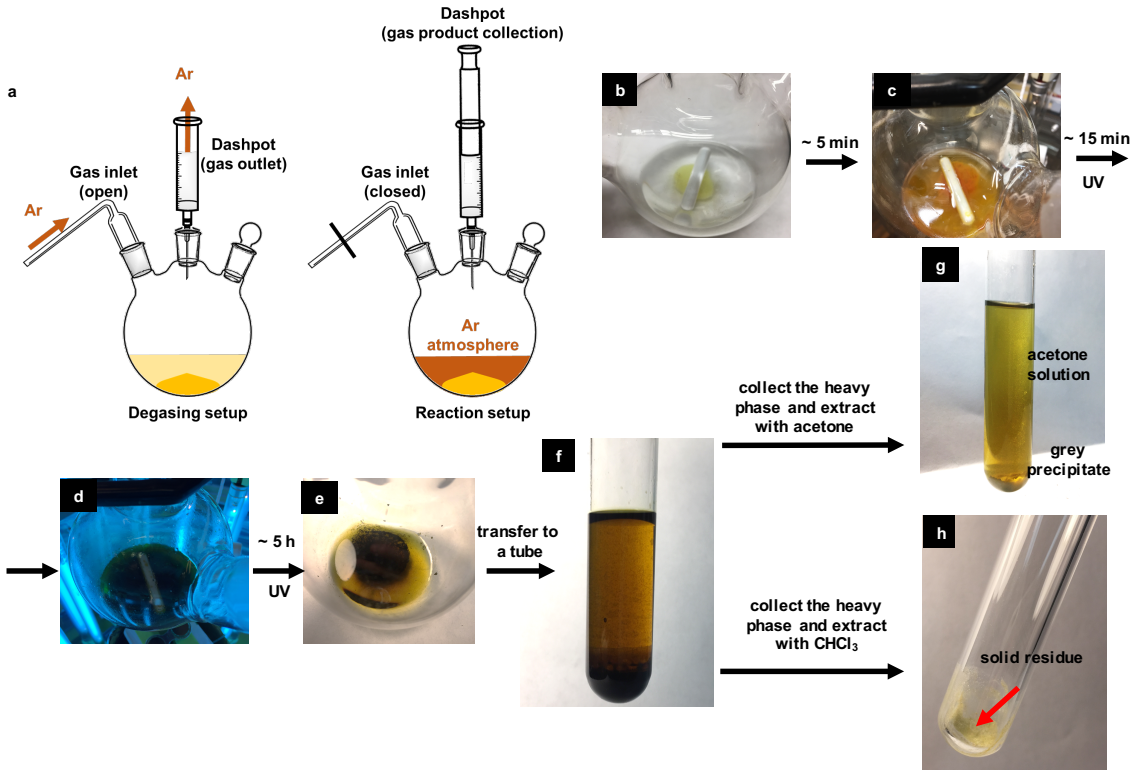

Figure S2. Experimental setup and photographs of PS degradation. (**a**) Setups for degassing and degradation-upcycling. (**b**) A mixture of $AlCl_3$, toluene, and PS in a three-neck quartz flask; (**c**) The mixture in **b** after stirring for ~ 5 min; (**d**) The mixture in **c** after exposure to a UV lamp for ~ 15 min; (**e**) The mixture in **d** after exposure to UV light for ~ 5 h. (**f**) A fraction of the light phase and heavy phase was transferred from **e** to a colorimetric tube. (**g**) The heavy phase in **f** was washed with acetone; (**h**) A part of the heavy phase in **f** was washed with chloroform.

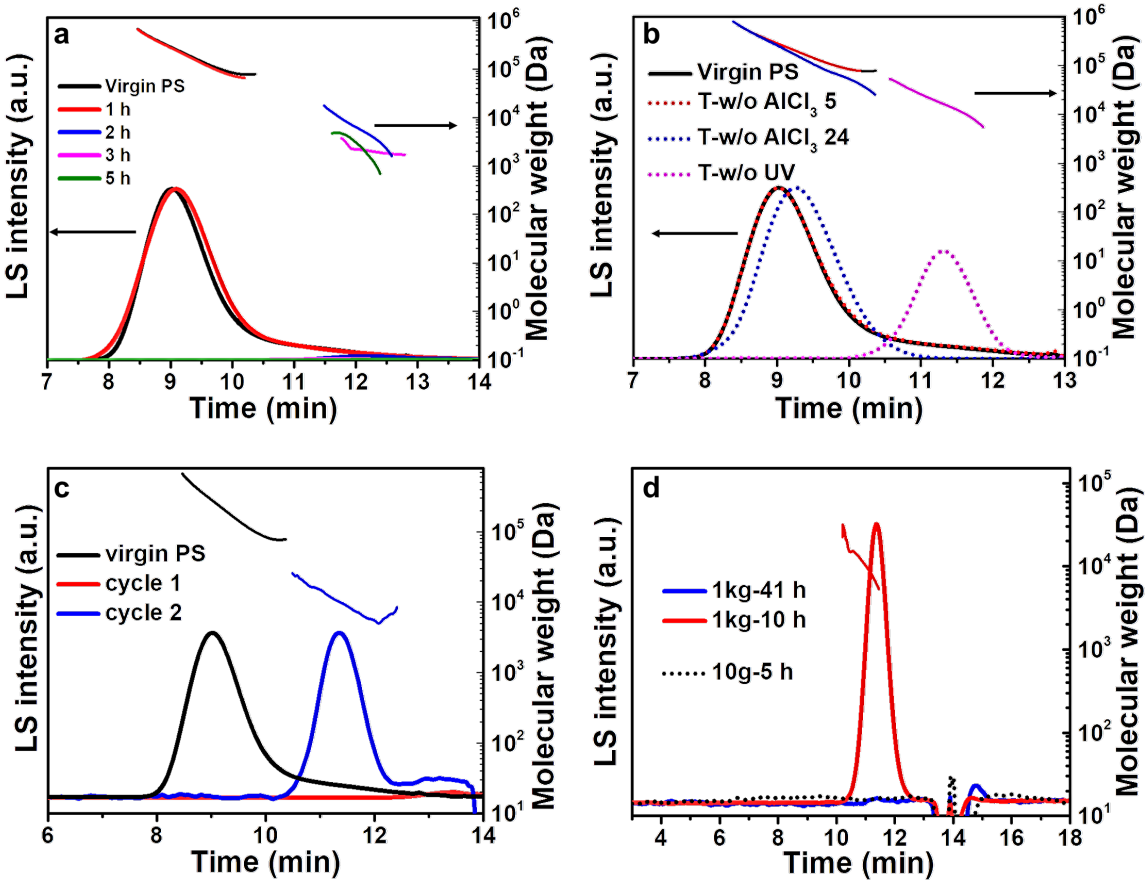

Figure S3. SEC analysis of PS after varying lengths of degradation time and under varying reaction conditions. (**a**) Virgin PS before and after photodegradation for 1, 2, 3, and 5 h. After 2, 3, and 5 h, the LS intensity was too weak to be detected and the traces were almost flat. (**b**) Control experiments of PS degradation. In T-w/o $AlCl_3$, the almost unchanged elution time indicated that PS barely degraded after 5 and 24 h. In T-w/o UV, the strong LS intensity but longer elution times show that PS was only partially degraded. (**c**) Reusability test of the catalysts. No fresh $AlCl_3$ was added after the Deg-Up cycle 1. In cycle 2, the reused catalyst was slightly less effective than fresh $AlCl_3$. (**d**) Batch degradation of 10-g PS foam after 5 h and 1-kg PS foam after 10 h and 41 h. No signal was detected after 41 h, which indicated complete PS degradation.

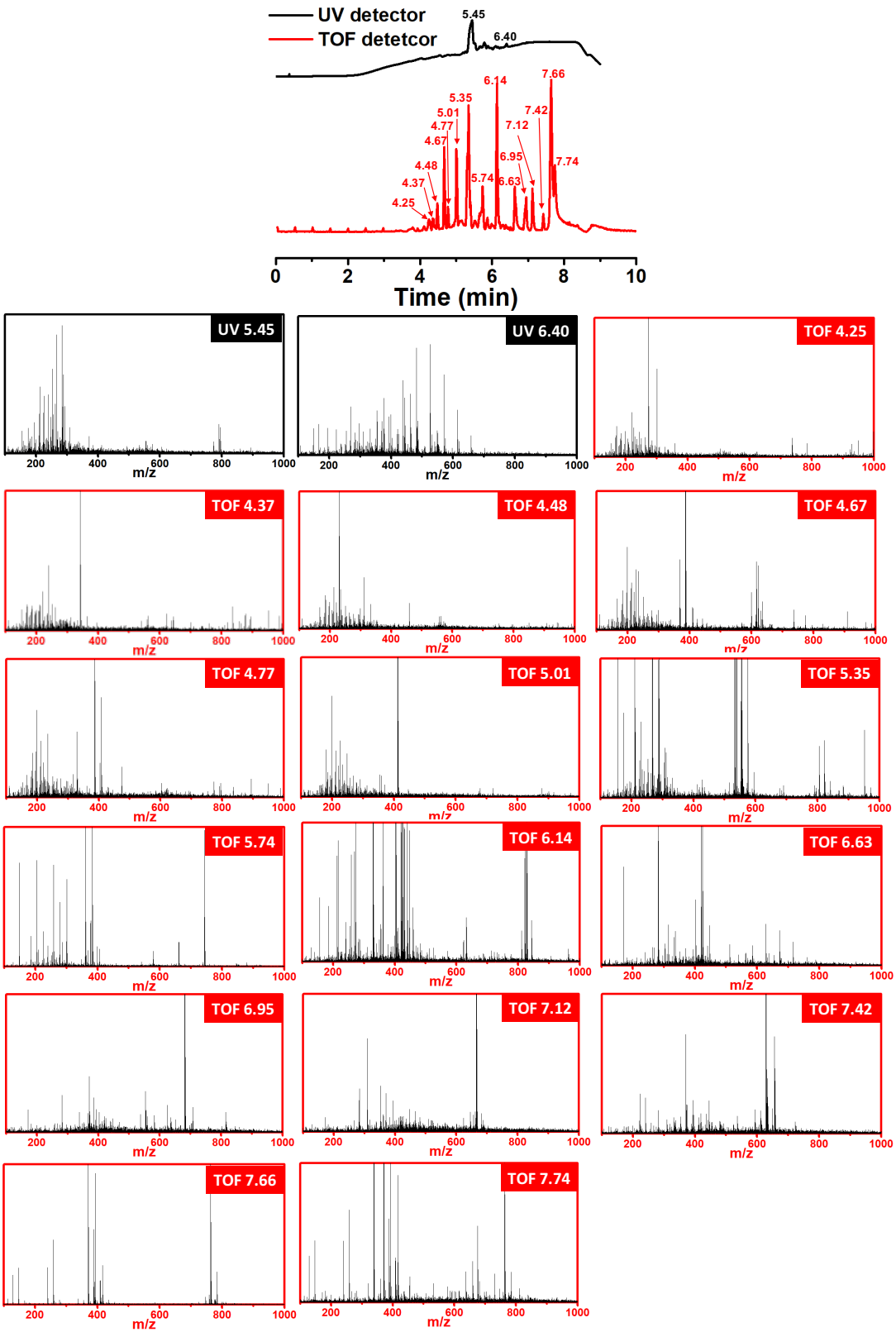

Figure S4. LC-MS of the mixture after PS degradation. (**a**) LC-MS traces determined by UV and Time-of-flight detectors. (**b**) Mass spectra of the eluents.

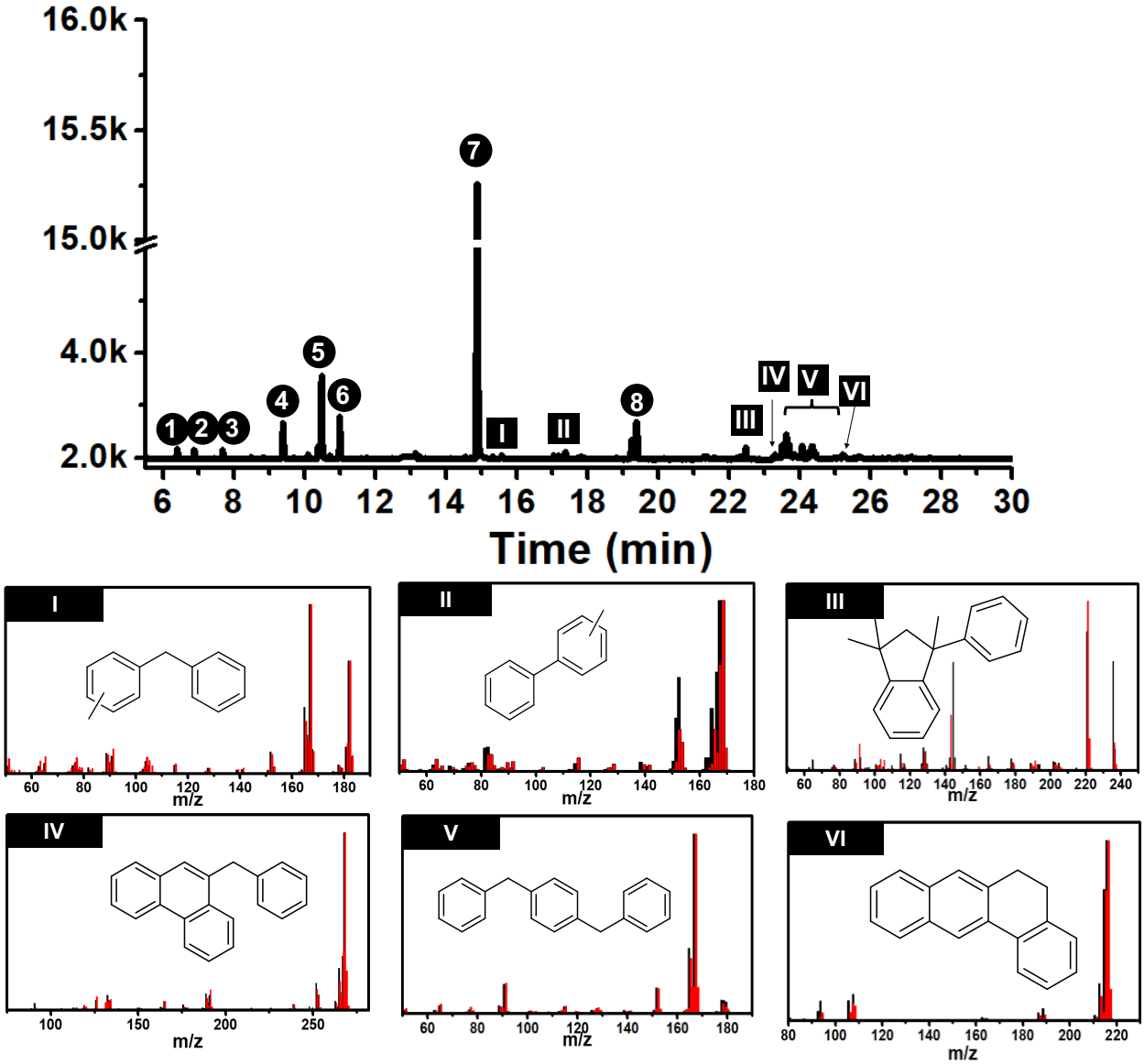

Figure S5. **Heavy aromatics after upcycling.** Solvents peaks are removed from the GC trace to draw focus to the minor side products. The fractions of products were evaluated by GC peak areas. Mass spectra of products 1-8 are shown in **SI Appendix, Figure S7**.

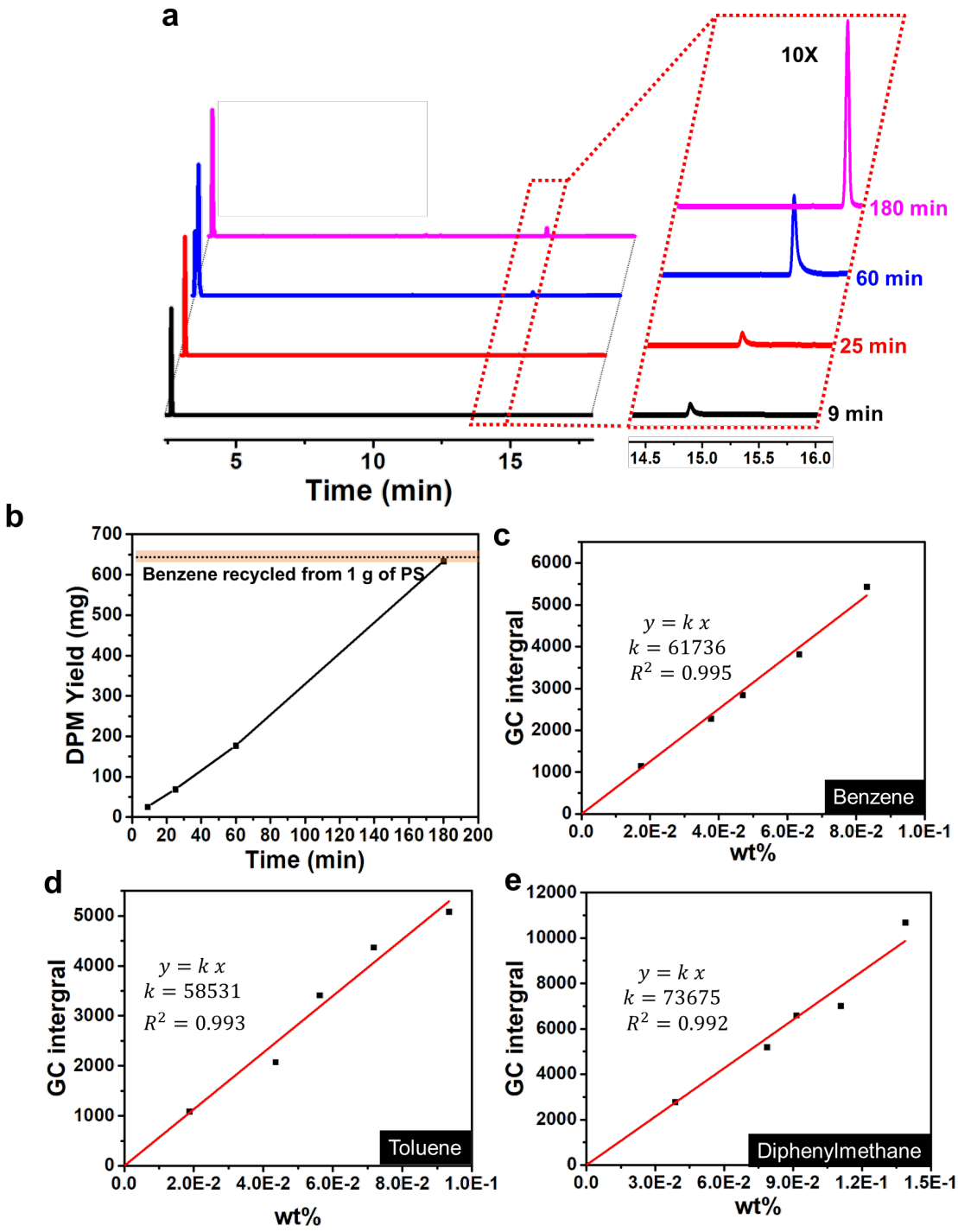

Figure S6. DPM upcycling as a function of time. (**a**) GC traces after various lengths of reaction time for DPM upcycling. The traces were normalized based on the benzene solvent signal at 2.7 min. The intensity of the DPM signal (at 14.7 min) increased with reaction time. (**b**) The relationship between the upcycling reaction time and DPM yield. The dotted line represents the amount of benzene recycled from 1 g of PS under our reaction conditions. The mass of DPM was calculated using **Equation (4)** and tabulated in **SI Appendix, Table S3**. Based on the DCM feed ratio in photodegradation and upcycling in benzene, we estimate that ~ 180 min was needed to upcycle all the benzene recycled from PS waste. (**c-e**) calibration curves of benzene, toluene, and diphenylmethane.

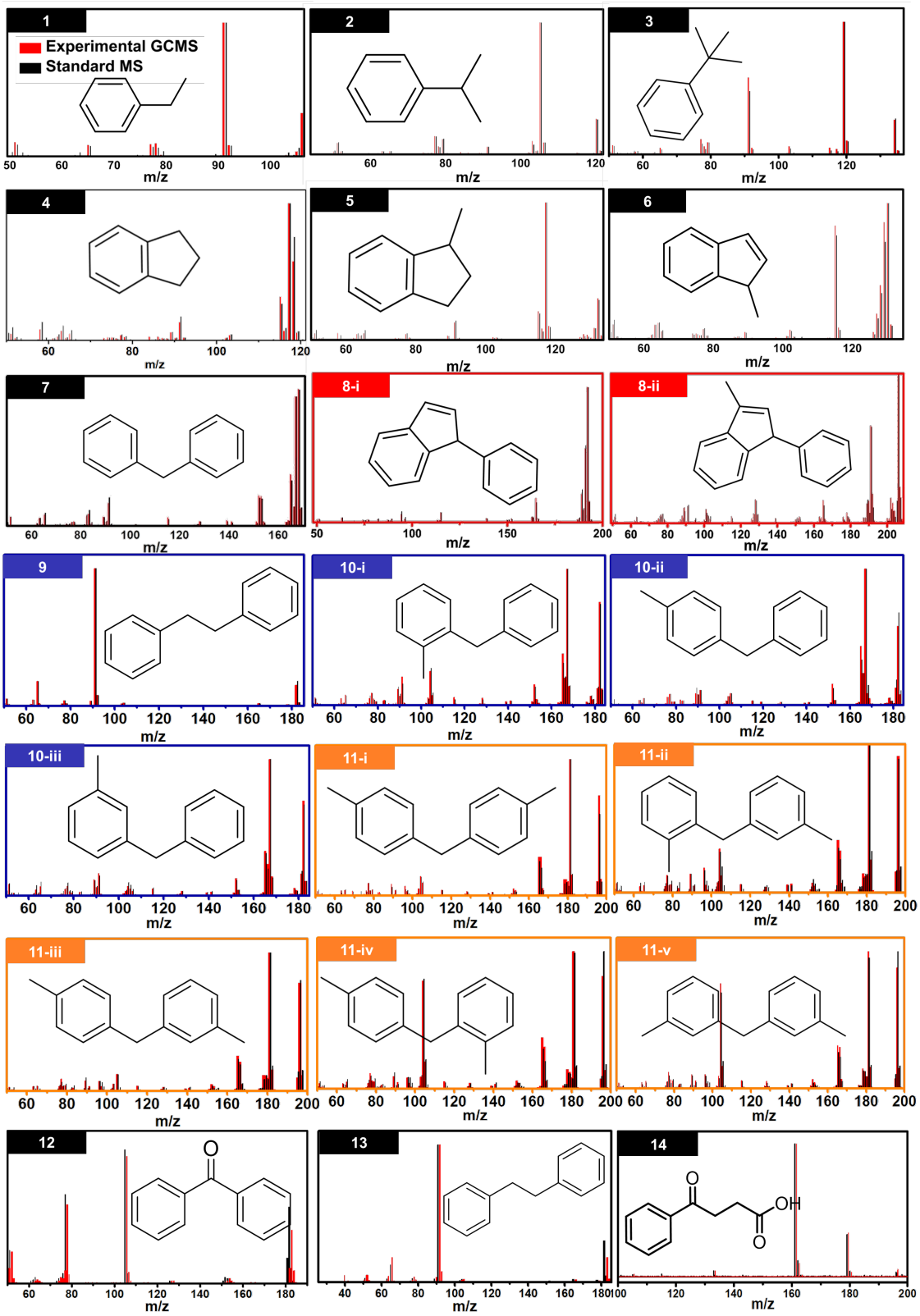

Figure S7. The MS spectra and corresponding chemical structures of the products, including isomers.

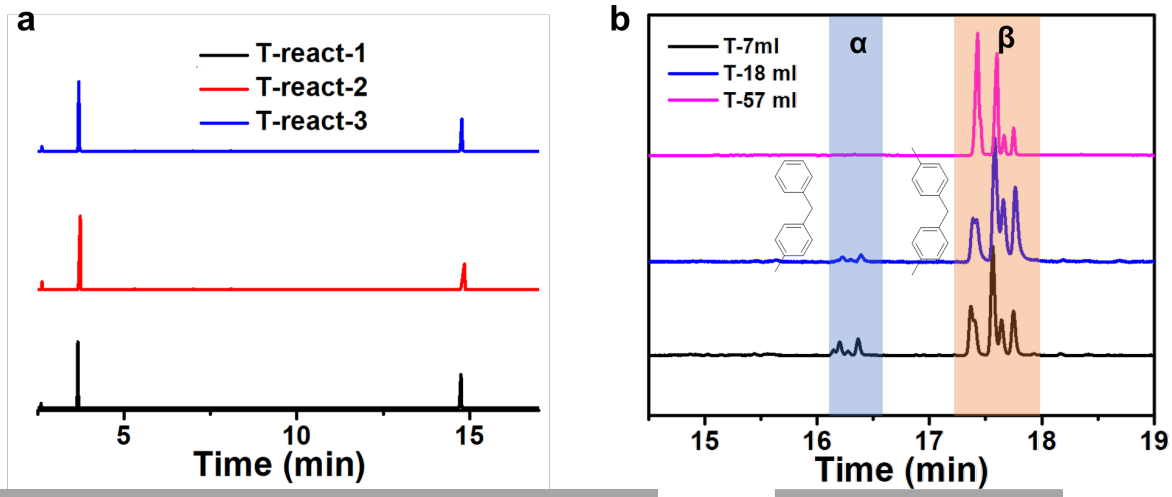

$m_{Tol,0}$ (mg)	m_{DPM} (mg)	Peak area ratio ($r_{Tol/DPM}$)	Δm_{Tol} (mg)	Solvent loss (%)
9890	7050	1.13	213	2.1
9880	4670	1.70	237	2.4
10200	6330	1.30	204	2.0

Volume of toluene (mL)	Peak area α/β
57	0.094
18	0.214
7	0.432

Figure S8. Solvent participation during degradation. (**a**) Solvent mass change during PS degradation was determined in the experiments using toluene as the solvent and DPM as an external reference for GC analysis. Three parallel experiments (T-react-1 to 3) were conducted. The changes in mass (2.2 wt. % on average) are attributed to both reacted and vaporized solvent. Therefore, the actual amount of solvent that participated in the degradation was lower than our estimate. (**b**) As the volume of toluene was increased, ditolylmethanes became the more dominant product over benzyltoluenes, as evidenced by the decreasing α/β peak ratio.

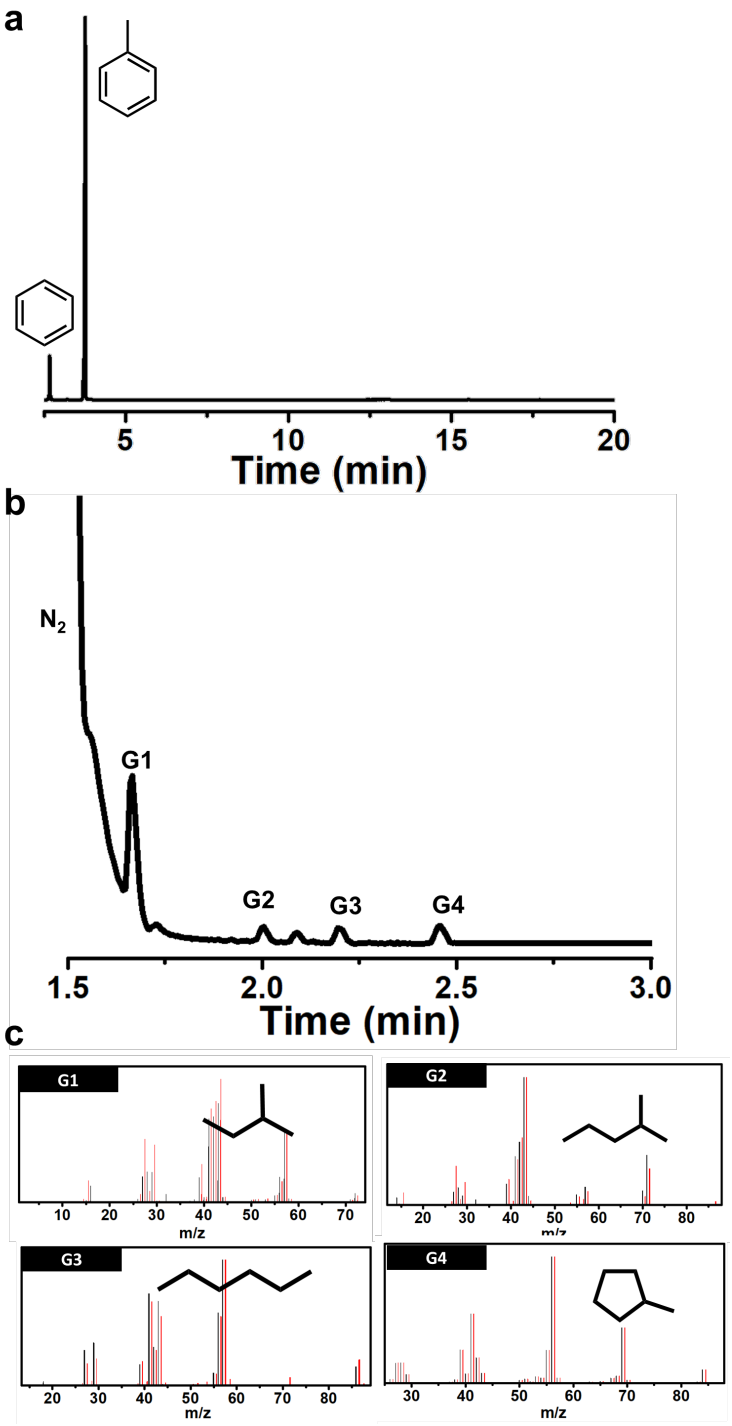

Figure S9. GC-FID and GC-MS analysis of the gas phase from the T-1 experiment. (a) GC-FID result of the gas phase shows primarily benzene and toluene. (b) GC-MS analysis of the gas phase reveals aliphatic volatile products; benzene signal at 2.7 min was not collected for clarity of the chromatogram.

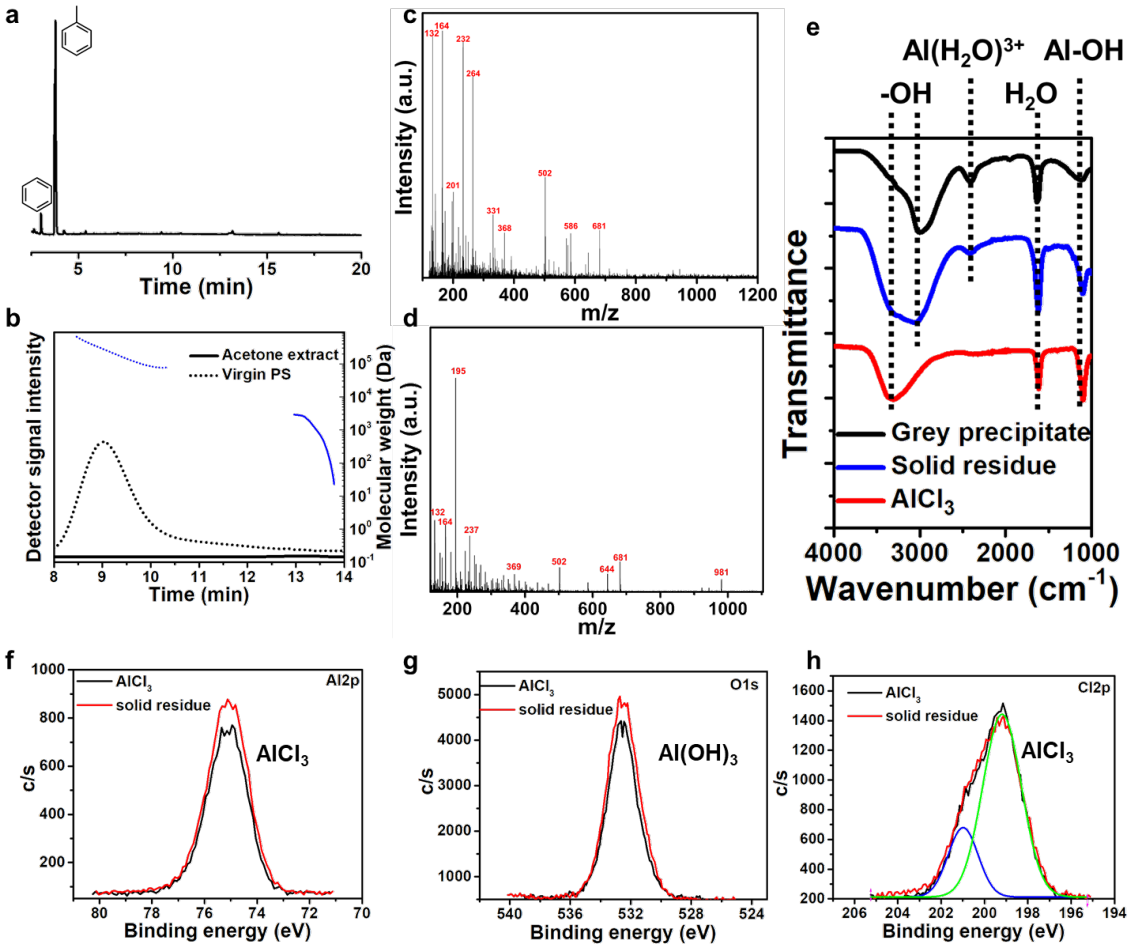

Figure S10. Characterization of acetone extract, grey precipitate, and solids residue. (**a**) GC and (**b**) SEC traces and (**c**) MS spectrum of the acetone solution in the T-1 experiment. (**d**) MS spectrum and (**e**) FTIR spectra of the grey precipitate. Solid residue and commercial $AlCl_3$ are included for comparison. Peaks above 3000 cm^{-1} showed the existence of hydroxides in the grey precipitate. The stretching vibration near 2411 cm^{-1} corresponded to octahedral aluminum hydrate ($Al(H_2O)_6^{3+}$). Due to the hygroscopicity of the hydroxides, water bending at 1626 cm^{-1} was present in all samples.(16) Peaks at 1103 cm^{-1} were assigned to Al-OH bending.(17) Therefore, the grey precipitate was primarily a mixture of aluminum hydroxides. The solid residue had a similar spectrum as the commercial $AlCl_3$, therefore the solid residue may contain unreacted $AlCl_3$. (**f-h**) XPS of the solid residue in comparison with $AlCl_3$. Al 2p and O 1s spectra indicated that solid residue is partially hydrolyzed, similar to $AlCl_3$. Cl 2p spectra confirmed the presence of $AlCl_3$ in the solid residue; the shoulder (201 eV) may be caused by hydrolyzation.

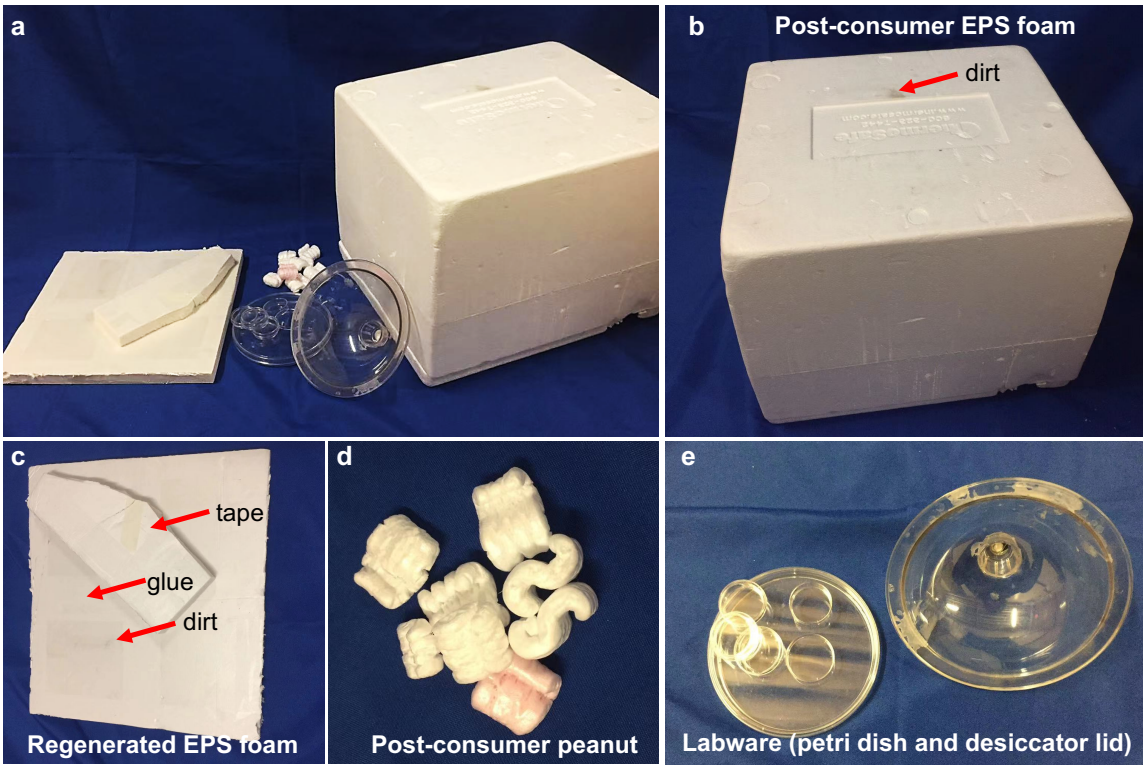

Figure S11. (**a**) A group photograph of post-consumer PS products employed for our Deg-Up reactions. (**b-e**) Zoom-in photographs of the PS wastes to highlight their low quality. (**b**) An expanded polystyrene (EPS) foam with dirt on the surface. (**c**) A regenerated EPS foam (produced from recycled PS) with glue, dirt, and tape on the surface. (**d**) PS peanuts with various dyes. (**e**) Common laboratory consumables and supplies made of PS, including Petri-dishes of different sizes and a desiccator lid.

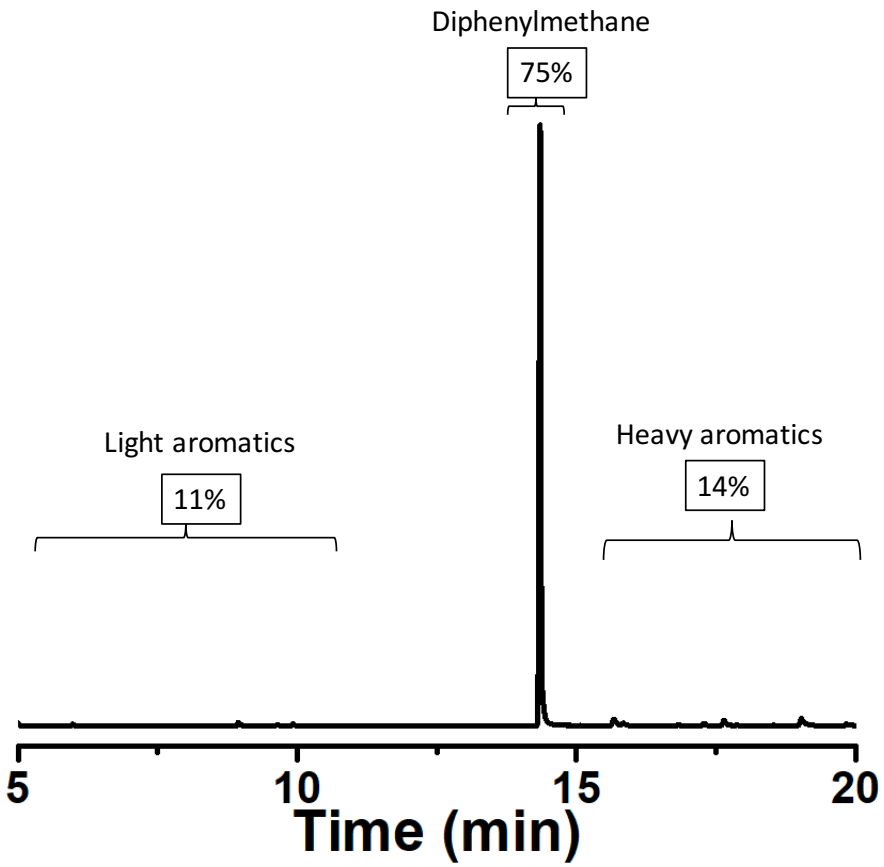

Figure S12. **The fractions of light aromatics, DPM, and heavy aromatics after upcycling 1 kg PS wastes and quenching with ice water.** The solvents are removed from the GC trace to draw focus to the products. The fractions of products were evaluated by GC peak areas.

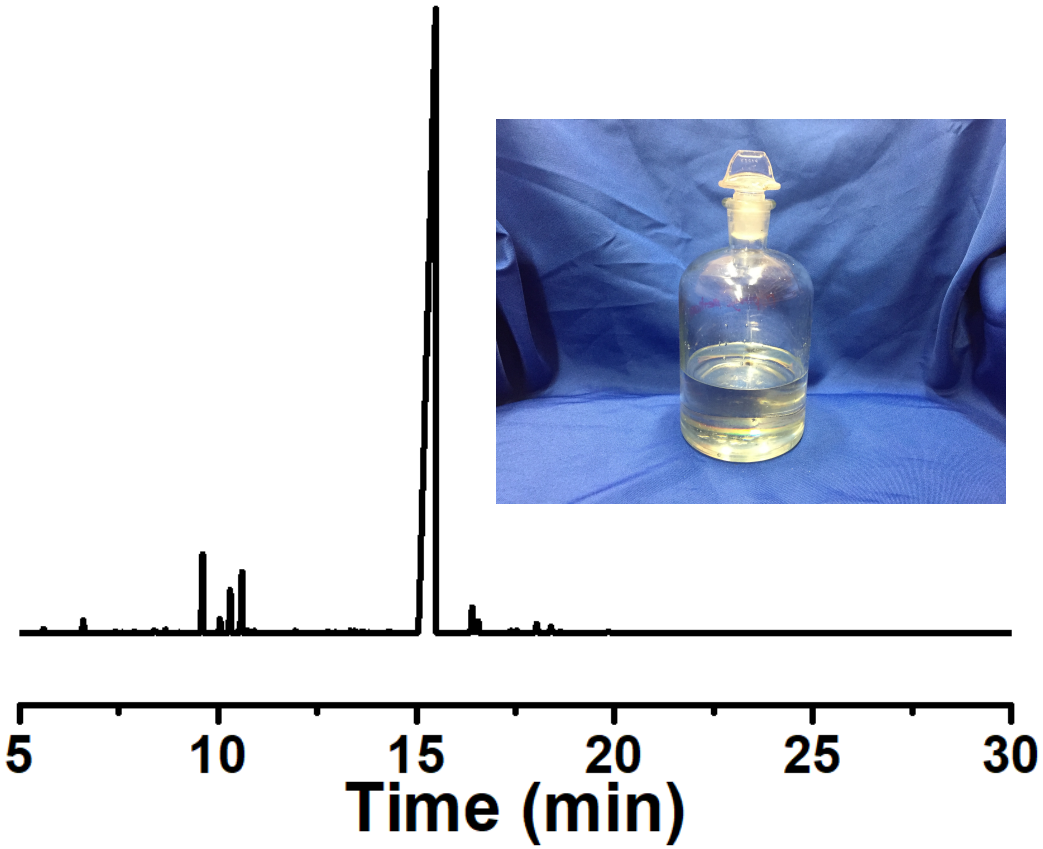

Figure S13. GC trace of DPM after one distillation step of the products from the 1 kg reaction. The GC traces represents the purity of DPM after distillation under vacuum. Only a small number of light and heavy aromatics are present in the product. (insect) The clear color of the liquid shows good purity.

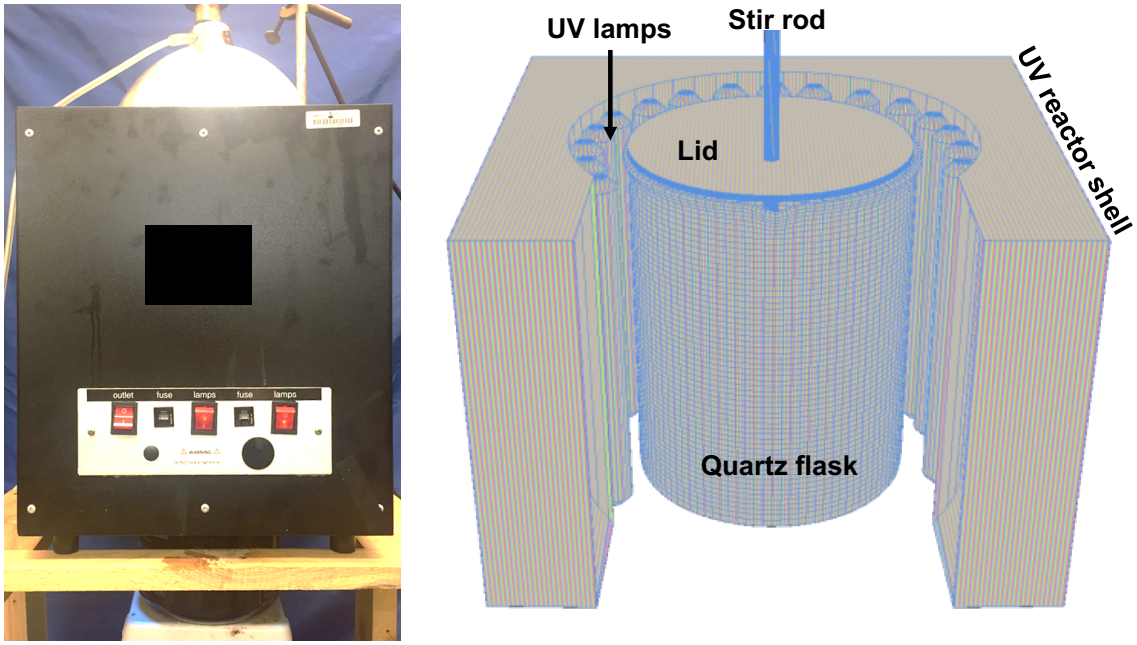

Figure S14. (left) A photograph and (right) scheme of a custom-built batch photoreactor. UV light transmittance of the quartz flask is ~ 70%. An aluminum foil lid was added to cover the reactor. A continuous Ar flow (100 mL/min) was applied to keep low levels of oxygen and moisture in the reactor.

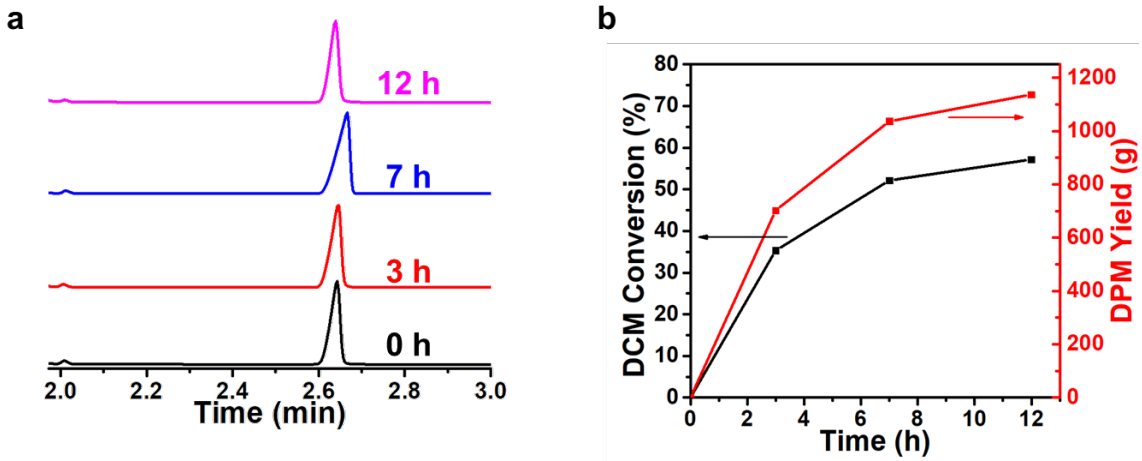

Figure S15. DCM conversion in the 1-kg scale upcycling reaction at room temperature. (**a**) GC traces of the upcycling solution after 0, 3, 7, and 12 h. (**b**) DCM conversion and DPM yield in the 1-kg batch Deg-Up reaction at room temperature. The conversion of DCM after 12 h was ~ 60 %.

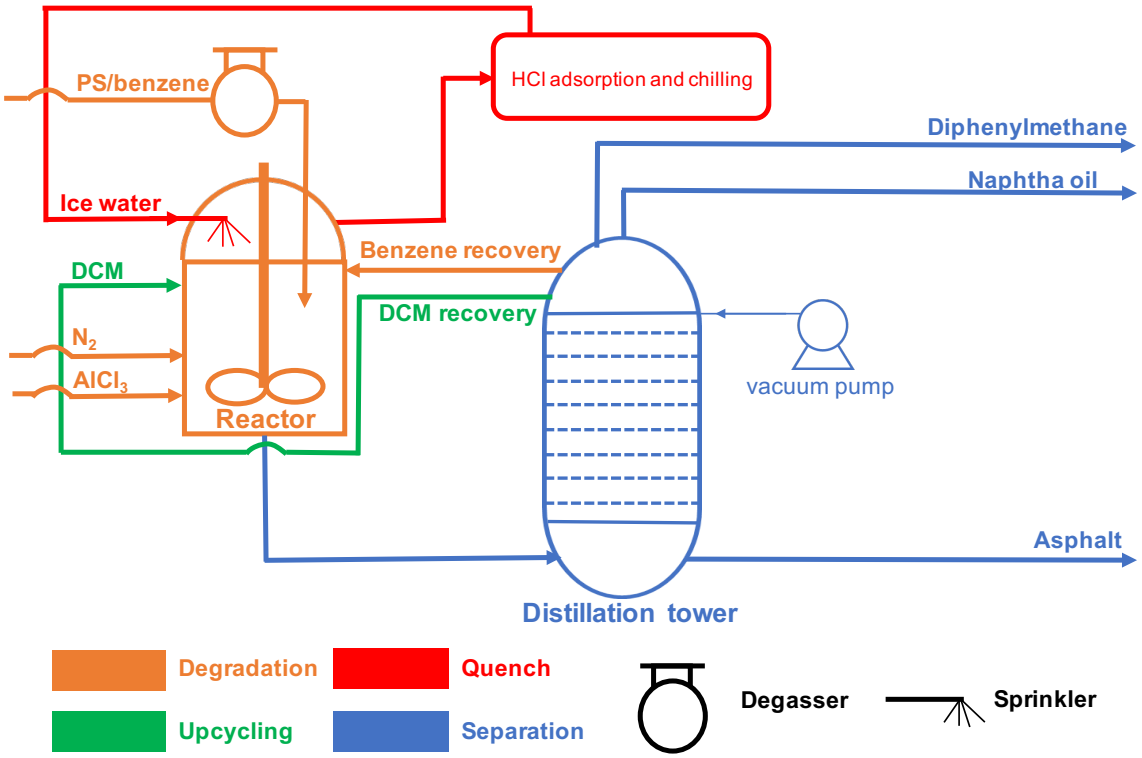

Figure S16. Graphical representation of the process flow design (PFD) for PS Deg-Up reaction at a 1-ton scale. Degradation, upcycling, and quenching steps are all completed in the reactor. The products are separated in the distillation tower, including the primary product of DPM and minor products of naphtha oil and asphalt. Benzene is recovered and fed back to the reactor to ensure sustainable upcycling circuitry.

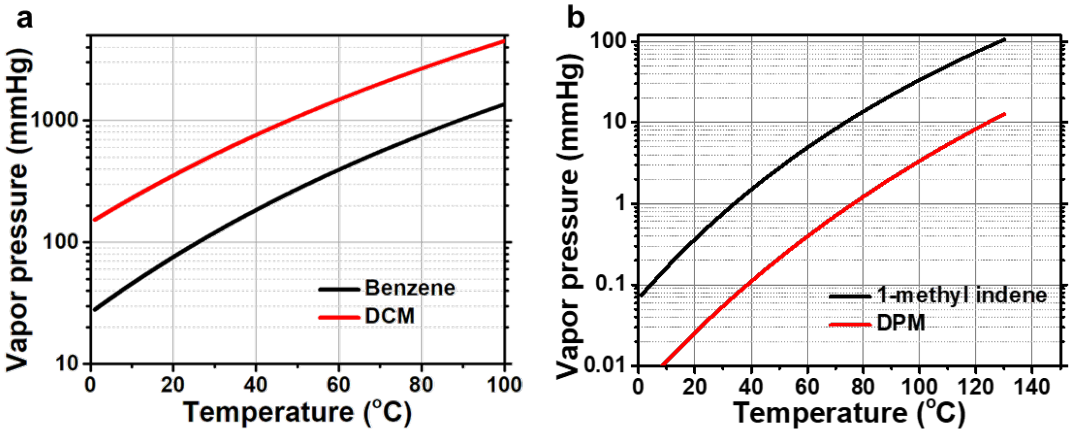

Figure S17. Vapor pressure of benzene, DCM, 1-methyl indene, and DPM. (**a**) Vapor pressures of DCM and benzene at varying temperatures are calculated according to the NIST database. (**b**) Predicted vapor pressure of 1-methyl indene and experimental vapor pressure of DPM at varying temperatures.(18)

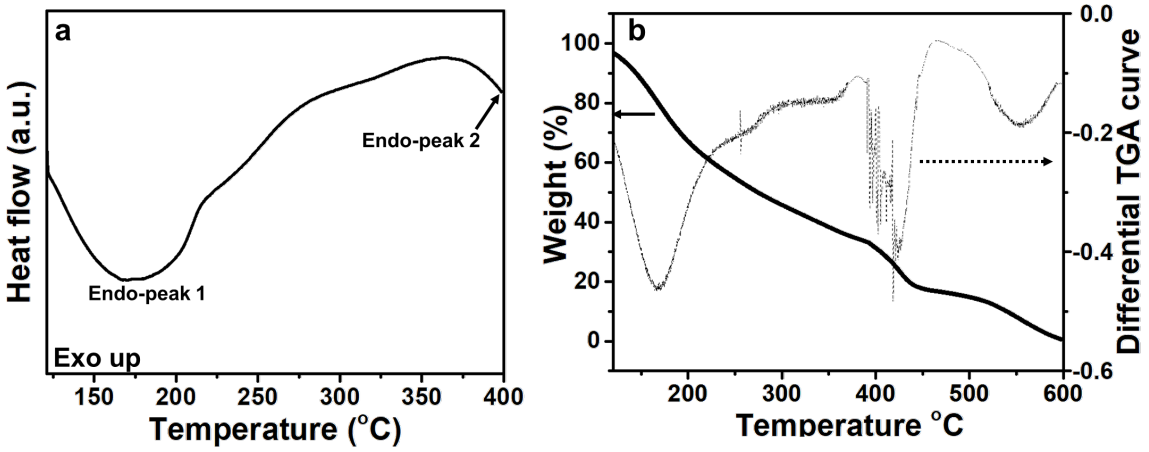

Figure S18. Thermal properties of the mixture after the upcycling reaction. Boiling points were evaluated by (**a**) differential Scanning calorimetry (DSC) and (**b**) thermogravimetric analysis (TGA). The first endothermic peak in DSC was attributed to both light aromatics and DPM. The second endothermic peak was assigned to asphalt. The first peak in TGA was attributed to the vaporization of solvents, light aromatics, and DPM, as confirmed by DSC. The second group of peaks (~ 400 ℃) corresponded to the vaporization of asphalt and degradation of some compounds.

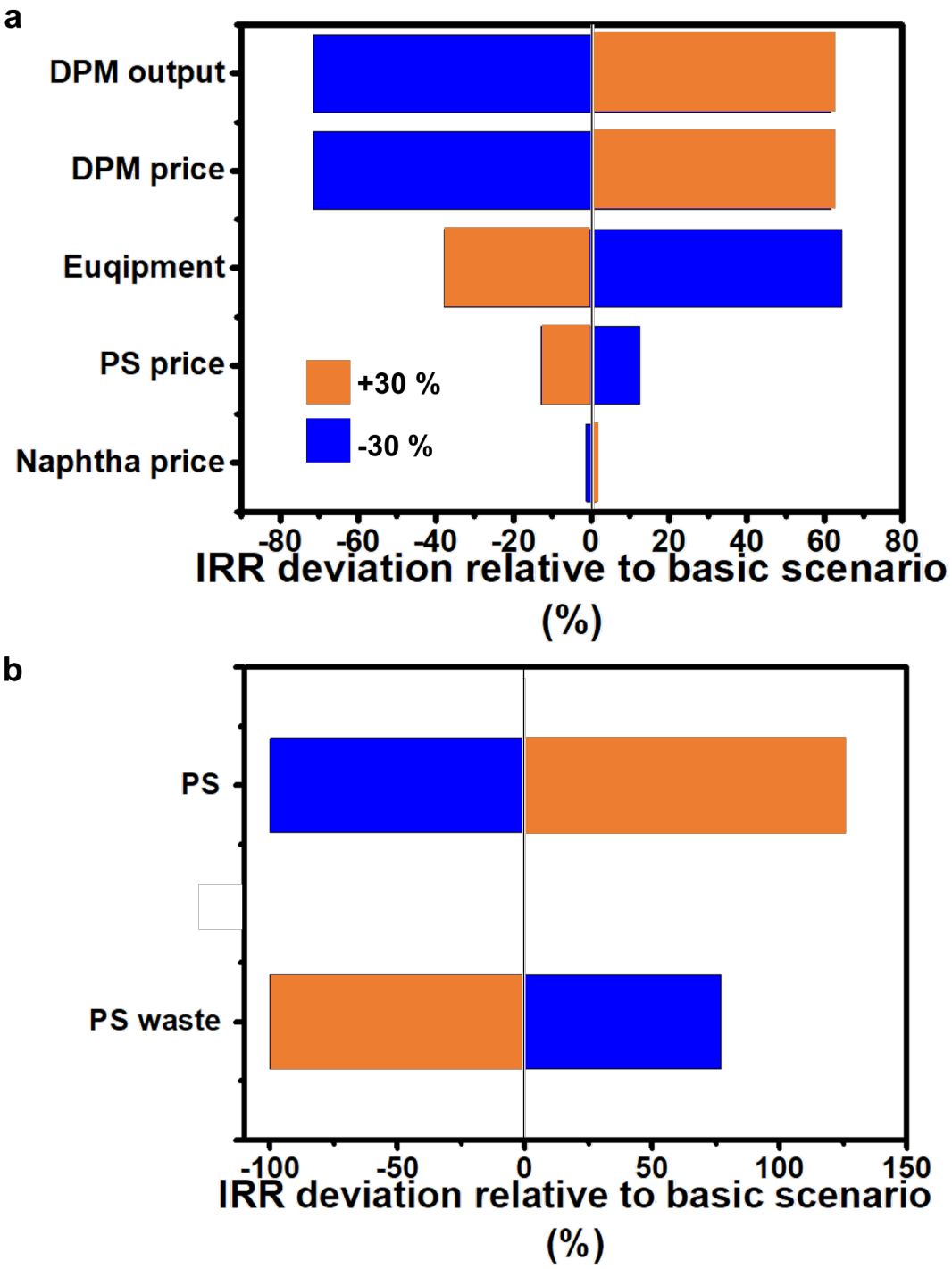

Figure S19. Tornado diagram illustrating the sensitivity analysis of (a) PS Deg-Up to DPM and (**b**) PS decomposition to styrene. The horizontal bars show the deviation of the IRR to the basic case.

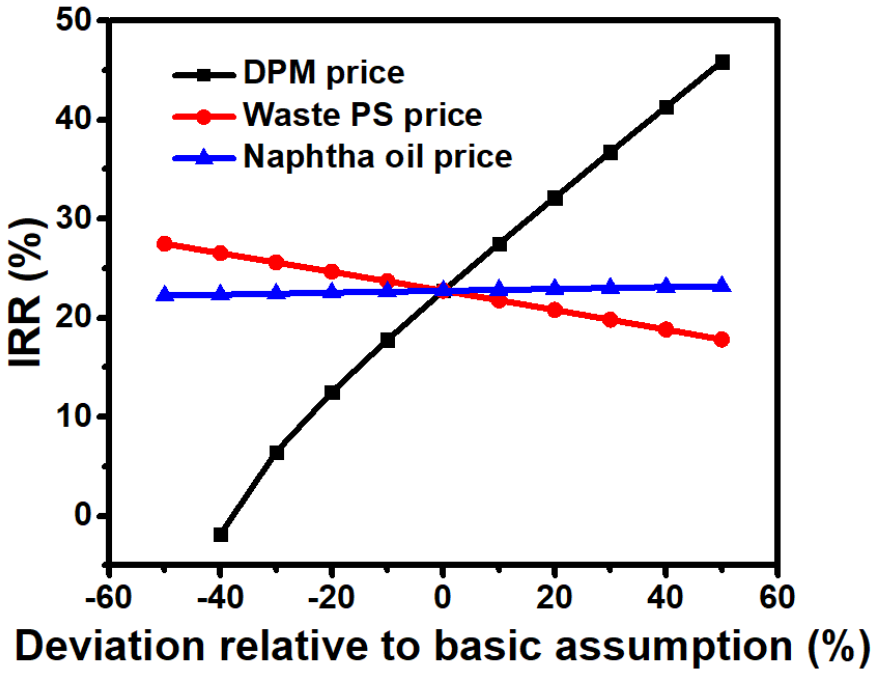

Figure S20. Sensitivity of IRR with respect to prices of DPM, waste PS, and Naphtha oil.

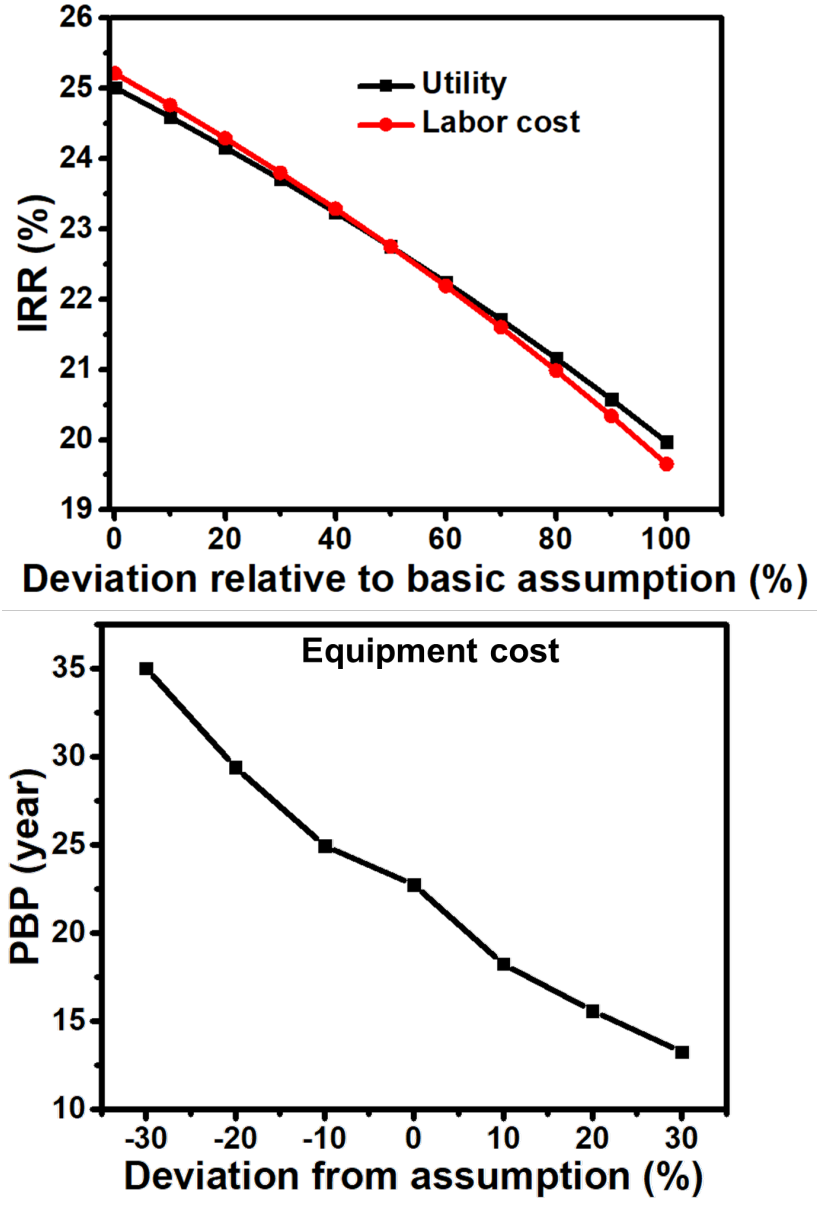

Figure S21. **Sensitivity analysis of utility, labor cost, and equipment cost.** Sensitivity analysis of (top) IRR with respect to utility and labor cost, ranging from 10% to 20% of the product cost and (bottom) PBP with respect to equipment cost, ranging from -30% to 30% of the basic assumption.

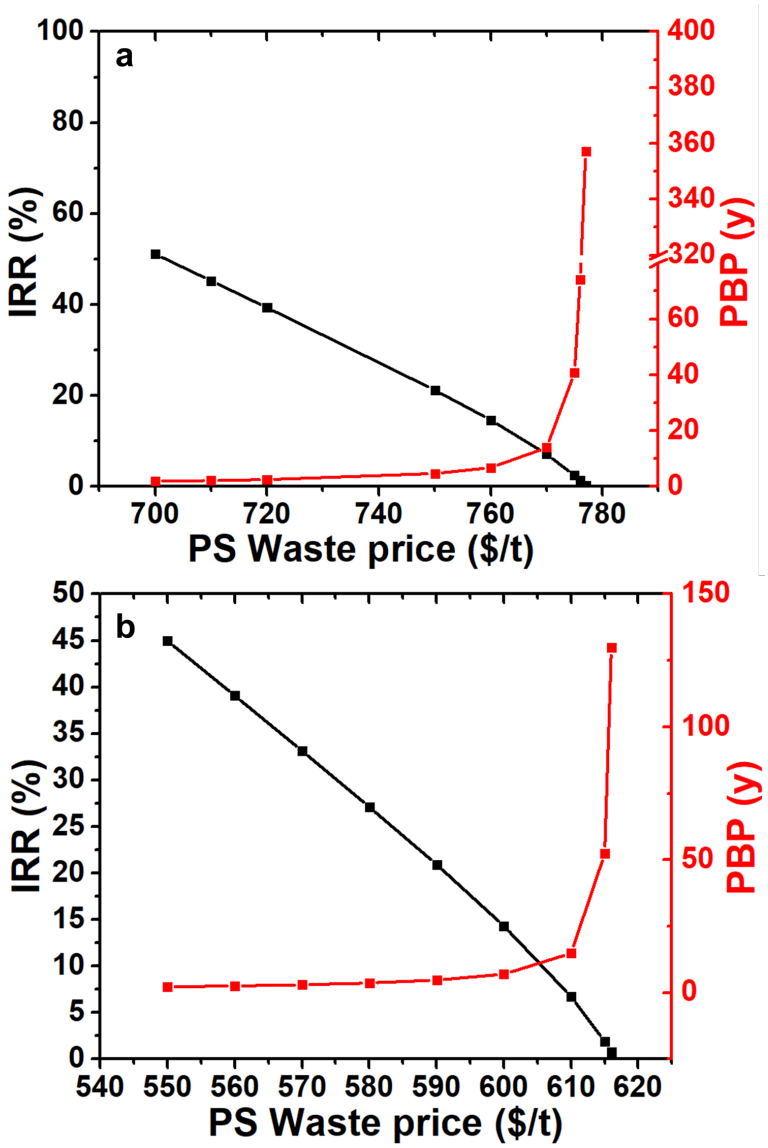

Figure S22. Sensitivity analysis of PS decomposition to styrene subjected to changes in the PS waste price. The regenerated PS price is preset to (a) $1500/t and (b) $1200/t.

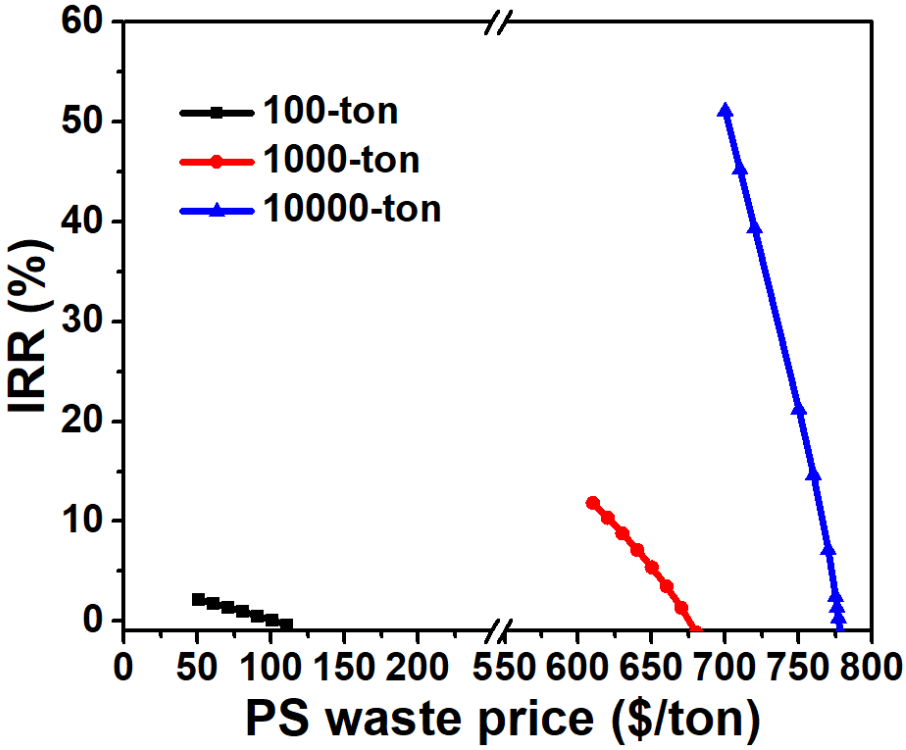

Figure S23. Effect of production scale on PS decomposition to styrene. Sensitivity analysis of IRR subjected to changes in PS waste price at annual capacities of 100, 1000, and 10000 tons. The process with an annual capacity of 10000-ton shows the steepest slope and thus the strongest sensitivity.

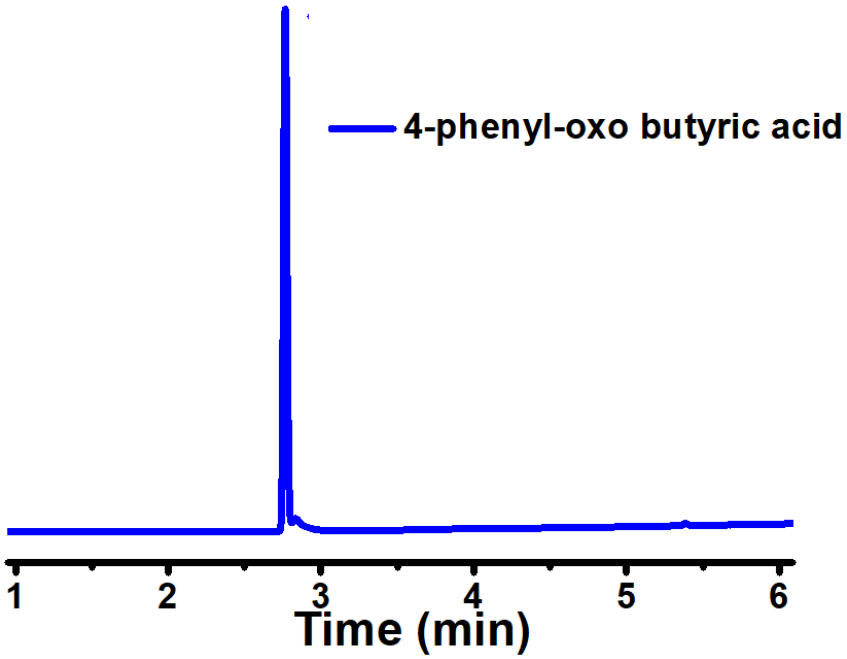

Figure S24: LC-MS traces of standard 4-phenyl-4-oxo butyric acid.

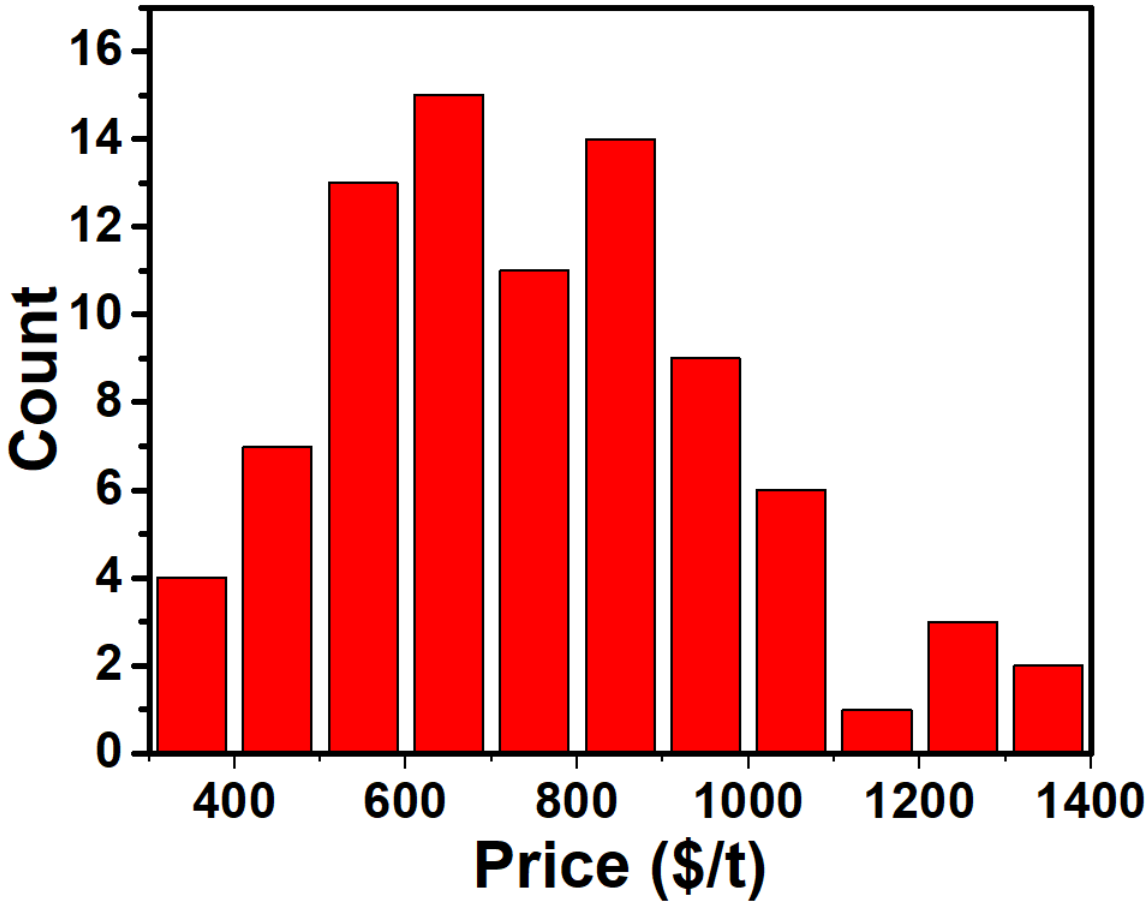

Figure S25. Price distribution of PS waste powders, granulates, and beads. The prices are collected from online sale platforms such as Alibaba, Indiamart, Recycler's world, and Scrapo in 15 countries.

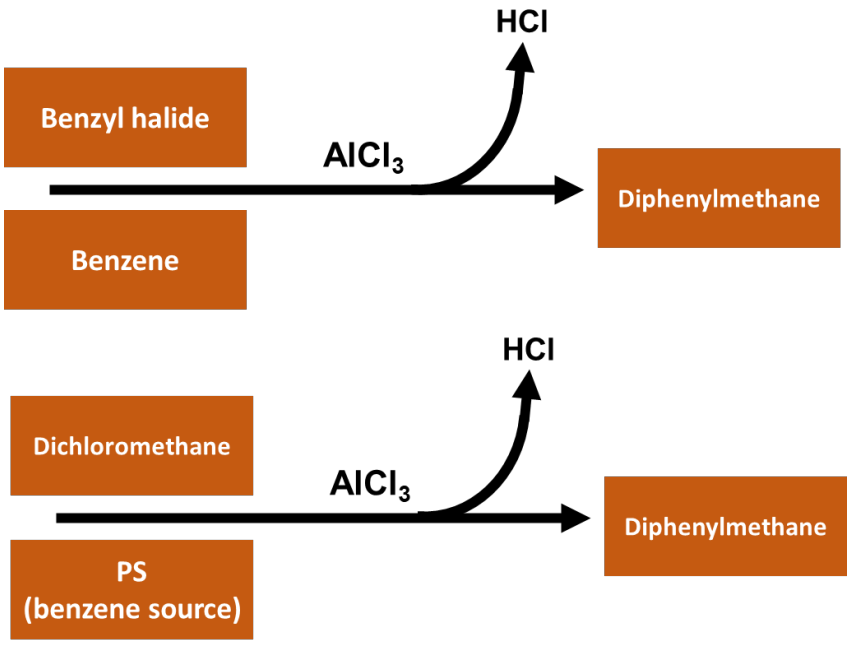

Figure S26. Comparison of our PS Deg-Up to DPM with an industrial DPM production process. Both processes have similar flows, primary products, and side products. The inputs of Deg-Up, however, are low-cost DCM and PS wastes.

Table S1. The feed, product phases, and benzene recovery

Designation [a]	Solvent	Reaction time (h)	Feed (g)			gas phase		light phase		heavy phase		Benzene yield [d]	
			PS	$AlCl_3$	solvent	g	wt. %	g	wt. %	g	wt. %	Mass (g)	Fraction (wt. %)
T-1	toluene	5	1.042	1.044	9.040	0.050	0.5	9.620	86.4	1.456	13.1	-	-
T-2	toluene	5	1.010	1.023	9.304	0.189	1.6	10.502	92.7	0.646	5.7	-	-
B-1 [b]	benzene	5	1.064	1.041	10.224	0.110	0.9	10.903	88.4	1.316	10.7	-	-
		5	1.010	0.876	4.576	-		-		-		0.685	68
		5	1.044	1.142	4.795	-		-		-		0.682	65
dB-1 [c]	D_6-benzene	0	0	0	1.412							-	
		5	1.010	0.832	8.596	-		-		-		0.665	67
dB-2 [c]	D_6-benzene	5	1.237	0.846	8.679							0.889	72

[a] Parallel experiments were designed in toluene (T), benzene (B), and deuterated benzene (dB) using a feedstock of PS (1) and waste PS foam (2).

[b] The mass of benzene was a sum of dissolved and gaseous benzene, calculated based on Equation (1). The mass of benzene in the gas phase and solution are also listed in **SI Appendix, Table S2**.

[c] The mass of benzene was determined based on Equation (3).

[d] The benzene yield was calculated based on the total mass of PS.

Table S2. Benzene yield from degradation of PS and waste PS foam.

	mass of reference (mg)	peak ratio ($r=A_{Ben}/A_{ref}$)	molar ratio (c)	mass of benzene (mg)		
				in solution	in vapor	total
T-ctrl[a]	9347	0	0	0	0	0
B-1[a]	1668	3.25	1	563	121.7	685
	1765	3.20	1	560	121.7	682
dB-1[b]	308	0.13	1	4.62	-	4.62
	2412	2.68	1	665	-	665
dB-2[b]	1503	5.63	1	889	-	889

[a] The reference chemical was toluene, and the peak ratios were obtained from GC traces. The mass of benzene was calculated based on Equation (1). The molar percent of benzene in B-1 was assumed to be unity.

[b] The reference chemical was chloroform, and the peak ratios were obtained from ^{1}H NMR. The mass of benzene in dB-1 and -2 were calculated based on Equation (3).

Table S3. DPM mass as a function of upcycling time.[a]

reaction time (min)	GC peak area		peak area ratio ($r=A_{DPM}/A_{Ben}$)	DPM mass[b] (mg)
	Benzene (A_{Ben})	DPM (A_{DPM})		
9	18400	52.0	0.00283	25.7
25	6540	50.0	0.00765	69.1
60	14000	272	0.0194	177
180	7160	499	0.0697	634

[a] Feedstock for Deg-Up was PS waste (1.010 g), $AlCl_3$ (0.999 g), and benzene (10.832 g).
[b] The mass of DPM was calculated based on Equation (4).

Table S4. Physical properties of the products.

	Name	Boiling point (℃)	Vapor pressure at 25 ºC (kPa)	Density (kg/m^3)
Volatiles	dichloromethane[a]	40	58.2	1330
	benzene[a]	80	12.7	876
Light aromatics	ethylbenzene[a]	136	1.28	866
	cumene[a]	152	0.61	862
	tert-butyl benzene[b]	169	0.29	860
	indane[c]	176	1.5	964
	1-methyl indane[d]	190	-	966
	1-methyl indene[a]	199	0.75	970
DPM	diphenylmethane[e]	264	0.05	1002
Heavy aromatics	tolyl phenyl methane[g]	278	6.22×10^{-4}	996
	p-methyl biphenyl[h]	268	0.0017	983
	1-methyl, 3-phenyl indene[f]	329	4.4×10^{-5}	1063
	3-phenyl indene[f]	318	8.72×10^{-5}	1092
	1,1,3-trimethyl-3-phenylindane[i]	163	1.64×10^{-4}	1018
	9-benzylphenanthrene[f]	452	-	1130
	1,4-dibenzylbenzene[f]	387	-	1040
	5,6-dihydrobenz[α]anthracene[e]	408	-	1150
Asphalt	pitch[j]	>400	-	-

[a] Physical properties are from *the CRC Handbook of Chemistry and Physics*.
[b] Physical properties are from the NIST database.
[c] Boiling point was recalculated based on reference (19).
[d] Boiling point and density are from literature, while vapor pressure is predicted by Advanced Chemistry Development (ACD/Labs) Software V11.02 (© 1994-2021 ACD/Labs).(20, 21)
[e] vapor pressure was recalculated from experimental measurement. (18)
[f] Properties were predicted by Advanced Chemistry Development (ACD/Labs) Software V11.02 (© 1994-2021 ACD/Labs).
[g] Boiling point and density were experimental values from the literature.(22)
[h] Boiling point was experimental value from the literature.(23)
[i] Boiling point and density were experimental values from the literature.(24, 25)
[j] Boiling point of the pitch was evaluated using the peak temperature in the differential TGA curve (**SI Appendix, Figure S18b**).

Table S5. Scale-up parameters for UV lamps

Photoreaction factors	values
$n_{1\ g}$	4.14×10^{23}
$n_{1\ kg}$	3.31×10^{24}
$\varphi_{1000/1}$	125
$n_{1\ ton}$	2.65×10^{25}
Experimental p_{ex}	0.0125 W·cm^{-2}
Commercial UV lamp p_{ex}	90×10^{-6} W·cm^{-2}
Commercial UV lamp illumination area	282,00 cm^2
$N_{1\ ton}$	94

Table S6. Distillation variables for light aromatics and diphenylmethane

	Items	Operation parameters	
		DCM-benzene	DPM
Distillation	Feed flow rate (F)	3.58 ton/h	1 ton/h
	Distillate mass flow rate (D)	0.62 ton/h	0.125 ton/h
	Bottom mass flow rate (B)	2.96 ton/h	0.875 ton/h
	Vapor flow rate (V)	0.218 m^3/s	123 m^3/s
	Dew point volatility (α_D)	4.11	11.72
	Bubble point volatility (α_B)	3.51	8.59
	Average relative volatility (α)	3.80	9.98
	Minimal reflux ratio	1.79	0.8
	Actual reflux ratio (R_{actual})	2.68	1.2
	Minimal stage number (N_{min})	5	4
	Column efficiency (E)	43%	20%
	Actual Tray number ($N_{T,actual}$)	12	20
	Average molecular weight of vapor phase (M)	83 g/mol	151 g/mol
	Density of liquid phase (ρ_L)	953 kg/m^3	964 kg/m^3
	Density of vapor phase (ρ_v)	2.90 kg/m^3	0.0006 kg/m^3
	Upper limit of vapor velocity (u_v)	3.07 m/s	228 m/s
	Minimal column area	0.07 m^2	0.55 m^2
	Actual column area	0.14 m^2	1.07 m^2
	Minimal Trey diameter (d)	0.42 m	1.17 m
Reactor dimension	Reactor volume	6 m^3	
	Number of UV light bulbs	94	
Tower dimension	Wall thickness	9 mm	
	Shell mass	994 kg	
	Tower diameter	1.18 m	
	Tower volume (m^3)	2.52 m^3	
	Plate distance	0.2 m	
	Tower length	4 m	

Table S7. Key assumptions of capital investment

Fixed capital investments		
(1) Direct cost		
	Equipment	
	Other direct costs (specified as % of equipment cost)	
	Installation	20%
	Piping	20%
	Instrumentation and control	20%
	Building & Structure	30%
	Yard improvement	10%
	Service facilities	50%
	Land	5%
(2) Indirect cost (specified as % of direct cost)		
	Engineering & supervision	15%
	Legal expenses	2%
	Construction expenses	15%
	Contractor's fee	3%
	Contingency	10%
Working capital: 15% of fixed capital investment		

Table S8. Other key assumptions and the prices of input and output

Assumptions	
Project length	20 years
Salvage value	0%
Depreciation method	Straight line depreciation (allows equipment to be depreciated at a constant rate. Each year the depreciation factor is 1/n, where n is years of depreciation)
Depreciation period	10 years
Annual interest rate	3%
Fixed costs, raw material and product prices	remain constant over time
DPM price[a]	$10000/ton
Naphtha oil price[b]	$600/ton
PS waste price[c]	$800/ton
Benzene price[d]	$820/ton
$AlCl_3$[e]	$300/ton
DCM[f]	$580/ton
Operating labor	15% of total product cost
Operating supervision	10% of operating labor
Utilities	15% of total product cost
Maintenance and repairs	5% of fixed capital investment
Operating supplies	15% of maintenance and repairs
Laboratory charges	15% of operating labor
Royalties	4% of of TPC without depreciation
Plant overhead costs	5% of total product cost
General expenses	10% of total product cost

[a] DPM is not a bulk but a specialty chemical. Its price was based on the lowest price reported on Chembid® (Shaanxi Dideu Medichem Co., Ltd. $10/kg).
[b] Naphtha oil is not a bulk chemical. Its price was obtained from Statista® "Price of naphtha worldwide from 2017 to 2021". The price in 2021 was utilized.
[c] The PS waste price is based on **SI Appendix, Figure S25.**
[d] The benzene price was obtained from Platts Global Benzene Price Index (March 18th, 2021).
[e] The price of $AlCl_3$ was obtained from Alibaba® wholesale platform (Weifang Yukai Chemical Co., Ltd. Yubin brand).
[f] DCM was obtained from bulk chemicals information platform, Echemi market price & insight (May 10th, 2021).

Table S9. Key equipment cost evaluations

PS Deg-Up			
	number	Price each	Price total
Light bulb[a]	94	$8.4	$900
Reactor[b]	1	$193,400	$193,400
Plate	20	$379	$13000
Pressure vessel	1	$23,600	$23,600
Vacuum pump[c]	1	$700	$700
Others[d]	-	-	$69,180
Total cost ($)	-	-	$301,000

PS decomposition to styrene			
Annual capacity	**10000 ton**	**1000 ton**	**100 ton**
Static mixer	$2,100	$1,700	$1,400
Pyrolysis reactor	$199,000	$105,000	$80,000
Polymerization reactor	$251,000	$119,000	$80,000
Accessories	$135,000	$67,000	$48,000
Total	$587,000	$292,700	$208,000

[a] The number of UV-C light bulbs was extrapolated based on the photon number required for 1-kg scale degradation. The cost of each light bulb was obtained from the wholesale market (detail.tmall.com/ Philips®; Oct. 2021).
[b] The costs of the glass-lined reactor, plate, and pressure vessel were calculated using a method in the literature.(26)
[c] The cost of the vacuum pump was obtained from the wholesale market (mscdirect.com; GAST®; Oct. 2021).
[d] The cost of other auxiliaries (*e.g.*, valves, gauges, and sinks) were evaluated based on 30% of the total equipment cost. The cost for pipelines and their maintenance were evaluated as an item of direct cost.

SI References

1. K. Qiao, Y. Deng, Alkylations of benzene in room temperature ionic liquids modified with HCl. *J. Mol. Catal. A Chem.* **171**, 81-84 (2001).
2. G. Towler, R. Sinnott, *Chemical Engineering Design - Principles, Practice and Economics of Plant and Process Design* (Butterworth-Heinemann, ed. 2, 2012).
3. W. McCabe, J. Smith, P. Harriott, *Unit Operations of Chemical Engineering* (McGraw-Hill Education, ed. 7, 2004).
4. M. Nitsche, R. Gbadamosi, *Practical Column Design Guide* (Springer, ed. 1, 2017).
5. J. C. Crittenden, R. R. Trussell, D. W. Hand, K. J. Howe, G. Tchobanoglous, "Appendix B" in MWH's Water Treatment. (John Wiley & Sons, 2012), pp. 1857-1858.
6. T. A. Ryan, E. A. Seddon, K. R. Seddon, C. Ryan, "Industrial manufacture and uses" in Phosgene: And Related Carbonyl Halides. (Elsevier Science, 1996), pp. 167-221.
7. N. E. Alexandrou, Friedel–Crafts reaction of oxalyl chloride with pentamethylbenzene. *J. Chem. Soc. C*, 536-537 (1969).
8. M. Kerscher *et al.*, Thermophysical properties of diphenylmethane and dicyclohexylmethane as a reference liquid organic hydrogen carrier system from experiments and molecular simulations. *Int. J. Hydrog. Energy* **45**, 28903-28919 (2020).
9. M. Peters, K. Timmerhaus, R. West, *Plant Design and Economics for Chemical Engineers* (McGraw-Hill Education, ed. 5, 2003).
10. 9Dimen, *Global Diphenylmethane Market Research Report 2020-2024*. (9Dimen Research Diphenylmethane Research Center, 2021)
11. GlobalInfoResearch, *The Sales and Revenue Report of Global Benzophenone Industry in 2021.* (Global Info Research, 2022)
12. Benzophenone - Global Market Trajectory & Analytics. researchandmarkets.com/reports/5301651/benzophenone-global-market-trajectory-and (accessed 5/8/2022),(2022).
13. Qixun, *The Survey & Forcast report of Chinese Benzophenone Industry, 2021-2026*. (Qixun industrial research 2021)
14. B. Cavinaw *et al.*, Systems and methods for recycling waste plastics, including waste polystyrene, USUS010731080B1, (2020)
15. A. Zayoud *et al.*, Pyrolysis of end-of-life polystyrene in a pilot-scale reactor: Maximizing styrene production. *Waste Manag.* **139**, 85-95 (2021).
16. N. Le Bozec, D. Persson, A. Nazarov, D. Thierry, Investigation of Filiform Corrosion on Coated Aluminum Alloys by FTIR Microspectroscopy and Scanning Kelvin Probe. *J. Electrochem. Soc.* **149**, 403-408 (2002).
17. D. L. Teagarden, J. F. Kozlowski, J. L. White, S. L. Hem, Aluminum chlorohydrate I: Structure studies. *J. Pharm. Sci.* **70**, 758-761 (1981).
18. S. A. Wieczorek, R. Kobayashi, Vapor pressure measurements of diphenylmethane, thianaphthene, and bicyclohexyl at elevated temperatures. *J. Chem. Eng. Data* **25**, 302-305 (1980).
19. D. Ambrose, C. H. S. Sprake, The vapour pressure of indane. *J. Chem. Thermodyn.* **8**, 601-602 (1976).
20. L. Schaap, H. Pines, The Potassium-catalyzed Reaction of Olefins with Arylalkanes1. *J. Am. Chem. Soc.* **79**, 4967-4970 (1957).
21. I. N. Nazarov, L. N. Pinkina, Acetylene derivatives. XLIX. Mechanism of hydration and cyclization of vinyl-1-cyclohexenylacetylene into 1-methyl-4,5,6,7-tetrahydro-3-indanone. *Izvestiya Akademii Nauk SSSR, Seriya Khimicheskaya*, 633-646 (1946).
22. L. N. Petrova, O. V. Shvarts, Benzylation of aromatic hydrocarbons in the presence of activated clay. *Russ. J. Gen. Chem.* **20**, 2168-2172 (1950).
23. X. Shao *et al.*, Determination and characterization of the pyrolysis products of isoprocarb by GC-MS. *J. Chromatogr. Sci.* **44**, 141-147 (2006).
24. H. Pines, L. Schaap, Base-catalyzed Hydrocarbon Cleavage Reactions: A Novel Wurtz-type Reaction. *J. Am. Chem. Soc.* **80**, 4378-4381 (1958).
25. L. A. Morozov, I. F. Baev, Practical possibilities for the utilization of the by-products obtained from the joint manufacture of phenol and acetone for the preparation of new electrical

insulating liquids. *Tr. Khim. Khim. Tekhnol.* **3**, 130-136 (1960).
26. L. K. Boerner, One-pot method turns polyethylene into valuable detergent precursor. *C&EN* **98** (2020).